EVALUATING HYDROLOGICAL RESPONSES OF

GIDABO RIVER CATCHMENT TO CLIMATE CHANGE:

RIFT VALLEY BASIN, ETHIOPIA

IYASU LEMMA

A THESIS SUBMITTED TO

THE DEPARTMENT OF WATER RESOURCES ENGINEERING

SCHOOL OF CIVIL ENGINEERING AND ARCHITECTURE

PRESENTED IN PARTIAL FULFILLMENT OF THE REQUIREMENT FOR THE DEGREE OF MASTER'S IN WATER RESOURCES ENGINEERING

(SPECIALIZATION IN IRRIGATION ENGINEERING)

OFFICE OF GRADUATE STUDIES

ADAMA SCIENCE AND TECHNOLOGY UNIVERSITY

AUGUST 2021

ADAMA, ETHIOPIA

Evaluating Hydrological Responses of Gidabo River Catchment to Climate Change: Rift Valley Basin, Ethiopia

Advisor: - Dereje Birhanu (PhD)

A Thesis Submitted to

The department of Water Resources Engineering

School of Civil Engineering and Architecture

Presented in Partial Fulfillment of the Requirement for the Degree of Master's in Water Resources Engineering

(Specialization in Irrigation Engineering)

Office of Graduate Studies

Adama Science and Technology University

August 2021

Adama, Ethiopia

DECLARATION

I hereby declare that this Master Thesis entitled "**Evaluating Hydrological Responses of Gidabo River Catchment to Climate Change: Rift Valley Basin, Ethiopia**" is my original work. That is, it has not been submitted for the award of any academic degree, diploma or certificate in any other university. All sources of materials that are used for this thesis have been duly acknowledged through citation.

Iyasu Lemma ___________________________ August 10, 2021

RECOMMENDATION

I, the advisor(s) of this thesis, hereby certify that I have read the revised version of the thesis entitled "**Evaluating Hydrological Responses of Gidabo River Catchment to Climate Change: Rift Valley Basin, Ethiopia**" prepared under my/our guidance by **Iyasu Lemma** submitted in partial fulfillment of the requirements for the degree of Mater's of Science in Water Resources Engineering (Specialization in Irrigation Engineering). Therefore, I/we recommend the submission of revised version of the thesis to the department following the applicable procedures.

Dereje Birhanu (PhD) __________________________ August 10, 2021

APPROVAL PAGE

I, the advisor of the thesis entitled "**Evaluating Hydrological Responses of Gidabo River Catchment to Climate Change: Rift Valley Basin, Ethiopia**" and developed by **Iyasu Lemma**, hereby certify that the recommendation and suggestions made by the board of examiners are appropriately incorporated into the final version of the thesis.

Dereje Birhanu (PhD)	______________________	August 10, 2021
Advisor	Signature	Date

We, the undersigned, members of the Board of Examiners of the thesis by **Iyasu Lemma** have read and evaluated the thesis entitled "**Evaluating Hydrological Responses of Gidabo River Catchment to Climate Change: Rift Valley Basin, Ethiopia**" and examined the candidate during open defense. This is, therefore, to certify that the thesis is accepted for partial fulfillment of the requirement of the degree of Master of Science in Water Resources Engineering (Specialization in Irrigation Engineering).

______________________	________________	________________
Chairperson	Signature	Date
______________________	________________	________________
Internal Examiner	Signature	Date
______________________	________________	________________
External Examiner	Signature	Date

Signature Date Final approval and acceptance of the thesis is contingent upon submission of its final copy to the Office of Postgraduate Studies (OPGS) through the Department Graduate Council (DGC) and School Graduate Committee (SGC).

______________________	________________	________________
Department Head	Signature	Date
______________________	________________	________________
School Dean	Signature	Date
______________________	________________	________________
Office of Postgraduate Studies	Signature	Date

ACKNOWLEDGMENTS

I would first like to thank my thesis advisor Dereje Birhanu (PhD) of the School of Civil Engineering and Architecture at Adama Science and Technology University**.** The door to Prof. Dereje's office was always open whenever I ran into a trouble spot or had a question about my research or writing. He consistently allowed this paper to be my own work, but steered me in the right the direction whenever he thought I needed it.

Finally, I must express my very profound gratitude to my parents and especially to my sister Bilen Lemma for providing me with unfailing support and continuous encouragement throughout my years of study and through the process of researching and writing this thesis. This accomplishment would not have been possible without them.

TABLE OF CONTENTS

LIST OF TABLES

LIST OF FIGURES

LIST OF ABBREVIATIONS

CMIP: Climate Model Inter-comparison Project

CORDEX: Coordinated Regional Climate Downscaling Experiment

GCM: Global climate model

GHG: Greenhouse Gas

HEC-HMS: Hydrologic Engineering Center's Hydraulic Modeling System

IPCC: Inter-governmental Panel on Climate Change

RCM: Regional Climate Model

RCP: Representative Concentration Pathways

SDSM: Statistical Downscaling Method

SRES: Special Report on Emissions Scenarios

SWAT: Soil and Water Assessment Tool

SWAT-CUP: Soil Water Assessment Tool Calibration and Uncertainty Program

WGN: Weather Generator Model

ABSTRACT

Water resources are stressed due to population increase and urbanization. Moreover, the climate change is further affecting the hydrological cycle. Hence, understanding the effect of climate change on various components of the hydrological cycle and water resources is crucial for the management of this essential resource. In this study, we used a hydrologic model to study the impact of future climate on the Gidabo River Catchment. The hydrologic model was created using the Soil and Water Assessment Tool (SWAT) model and the SWAT-CUP for the sensitivity analysis, calibration and validations of model parameters using monthly river discharges at three subbasin level. Future climate scenarios for periods 2020's and 2050's were applied using the Bias corrected precipitation, maximum and minimum temperature data from the four regional climate models CCLM4, RCA4, RACMO22T, and REMO2009 under RCP 4.5 and RCP 8.5 as input for the hydrologic model. Correlations between streamflow and meteorological variables were investigated, while nonparametric tests were applied to determine the trends and correlations. For future scenarios a significant increasing trends of annual and monthly mean temperature is found about 0.76 °C for RCP4.5 and 0.85 °C for RCP8.5 in the 2020s, and by 1.78 °C for RCP4.5 and 2.3 °C for RCP8.5 in the 2050s for the mid-term period, whereas during the whole period the annual and monthly precipitation in the basin did not exhibit similar trends although temporal and spatial variations were detected. The result of this study will provide crucial information to water resource managers for decision makings that address the consequences of climate change.

Keywords: Climate Change, Streamflow, SWAT, CORDEX-AFRICA, and Trend Analysis

1. INTRODUCTION

1.1. Background

Climate change is undeniable and many of the changes that have been observed in decades or millennia since the 1950's are never before. The atmosphere and ocean warmed, snow and ice fell and the sea level rose (IPCC, 2014). The global mean surface temperature is expected to increase by the end of the 21st century (2081 to 2100), from 0.3 to 1.7°C, from 1.1° to 2.6° C under RCP4.5, from 1.4 to 3.1° F under RCP6.0, and from 2.6°C to 4.8° C under RCP8.5 as compared with 1986 – 2005 (IPCC, 2014). Climate change has a huge impact in many parts of the world on local and regional hydrological regimes (Dibike and Coulibaly, 2005).

The effects on society and natural resources of climate change depend on the reaction of the hydrological cycle to global warming (Marvel and Bonfils, 2013). It is important to remind ourselves of the principles of the hydrological cycle, which generate all hydrological components in the hydrological regimes. The hydrological cycle, which involves water that moves continuously from the ocean to the air and completes a cycle, includes precipitation, infiltration, percolation, runoff and evapotranspiration. This makes climate change a major cause of hydrological change (Marvel and Bonfils, 2013; Bhuvandas et al., 2014) and an influence on all processes that make up the hydrological cycle.

Climate change and variability are prevalent in both socio-economic and ecological systems, and this study was started to assess the negative and positive effects of current and predicted climate change and variability (M. Keller, 2009). It is critical to conduct research on climate change in the Gidabo basin in particular. As a result, the study examines the general trends of future climate variables such as precipitation, maximum temperature, and minimum temperature in comparison to the current situation, as well as the potential future impacts of climate change on the Gidabo River's stream flow at a regional scale using Regional Climate Model Outputs, RCPs, archived in CORDEX-Africa.

According to Giorgi et al., (2009), the Coordinated Regional Climate Downscaling Experiment (CORDEX) aims for a broad assessment of the regional implications of rising greenhouse gas (GHG) emissions in the next decades. Ethiopia's GHG emissions are inextricably linked to the population's basic food and heating needs. As a result, future GHG emissions are expected to increase in lockstep with population growth. Africa was chosen as one of CORDEX's target locations for three reasons: first, the region's high susceptibility in various sectors is due to climate unpredictability, second, the region's economies have comparatively limited adaptive capacity, and third, massive temperature changes abound in the region.

Furthermore, there are fewer models for Africa that use regional climate downscaling (RCD) methodologies. Regional climate models (RCMs) dynamically downscale GCM output to end-user scales, making them effective for understanding local climates in locations with complicated topography and accounting for land surface heterogeneity (Endris et al., 2013 and Gbobaniyi et al., 2014). RCMs can also be used to zoom in and out of climate data from a regional to a small scale (Akinsanola and Ogunjobi, 2017).

Ethiopia is one of the most vulnerable countries in terms of climate change and also has an important effect in many parts of the world on hydrological regimes. Several studies have evaluated the performance of multimodal numerical simulations and multi observational data bases focusing on seasonal cycles and spatial variations of precipitation over Ethiopia, such as (Diro et al., 2011; Endris et al., 2013; Haile and Rientjes, 2015; Jury, 2015; Reda et al., 2015; Worku et al., 2018; and Van Vooren et al., 2019). Most studies used internationally available gridded and satellite-based data sets as a reference to evaluate the CORDEX-Africa RCMs output.

The goal of this research is to determine how climate change will affect water availability and hydrological extremes in the Gidabo River basin. To accomplish so, we'll employ the SWAT Model, which will be forced by bias corrected climate model output from the CCLM4-17, RCA4, RACMO22t, and REMO2009 regional climate models, as well as the new IPCC scenarios RCP 4.5 and 8.5. The model simulations were used to estimate the susceptibility of hydrological extremes to climate change, quantify run-off, and seasonal fluctuations in river flow.

1.2. Statement of the Problem

Climate change's impact was a prominent issue in the global and local environmental issues. The effect of precipitation, evapotranspiration, and temperature on river runoff is a significant environmental element (nutrient transportation, sedimentation, and plant and fauna habitats), agricultural (drainage and flooding), and economic factor (e.g. Water supply, flooding, engineering, and agro-economics). As a result, a good prediction of future runoff is crucial in assessing the situation regarding climate change's impact (Shanka A.S., 2017).

The climate in the Gidabo River Basin was extremely changeable, and the mountains on the cliffs progressively changed from semi-arid in the rift floor to humid in the rift floor. Rift floor precipitation is greater than 1,600 mm/year in mountains and climbs, while the lowest height on the rift floor is less common, often less than 800 mm/year. The precipitation had a subordinate peak in September and October due to the bimodal pattern of April and May (low rain season) (heavy rain season). The basin's temporal and geographical temperature shifts were more noticeable than seasonal swings, as they were throughout Ethiopia.

As a result, the country's minimum temperature has risen by 0.37°C each decade to 0.4°C. While temperature increases were large and reasonably consistent across locations and over time, precipitation changes were more confusing, with different sources reporting different figures. When averaged over the country, precipitation has been relatively consistent during the last 50 years, with the exception of a decline in July-September rainfall in the 1980s, which has since rebounded in the 1990s and 2000s. However, these averages do not reflect local conditions, which were widely varied, and the country's intrinsic fluctuation in rainfall makes detecting long-term patterns difficult (Keller M., 2009).

The future is inherently unknown, which is partially mitigated by emission scenarios that represent several ideas of how the world will evolve in terms of population, technology, and energy use in the future. Despite the fact that significant research has been done on climate change at the continental or global size, the degree and kind of impact at the regional-catchment scale has not been examined in many places of the world, including Ethiopia.

1.3. Research Objective

General Objective

The overall objective of this research was to evaluate the hydrological responses of the Gidabo River Catchment to climate change using the SWAT hydrological model.

Specific Objectives

- Calibrating and validating the SWAT hydrological model and to assess the best model parameters that affect the hydrological process significantly.
- Assessing the probable trends in precipitation and temperature in the future compared to the baseline period.
- Evaluating the current and future water availability at the watershed in 2020's and 2050's under changing climate.

Research Questions

The main and specific objectives of this study were derived from research questions relevant to evaluating the hydrology of Gidabo River Catchment. Therefore, the current study addresses the following research questions:

1. Which model parameters affect the hydrological process and the performance of SWAT hydrological model significantly?
2. What is the likely trend in temperature and precipitation in the near future 2030 to mid-term 2060 compared to a baseline period?
3. How the water availability will likely change in the future compared to the baseline period?

1.4. Significance of the Study

According to Ethiopia's 2018 Climate Change Profile, the region receiving adequate precipitation during the Belg season has reduced by 16 percent since 1990. Kiremt rain is decreasing in the same portions of the country, primarily in densely populated Rift Valley districts in the SNNPR and south/east Oromia provinces. About 20 million people live in the affected areas, who are facing chronic food insecurity as rainfall levels fluctuate from "just enough to support agricultural production" to "insufficient, resulting not harvest failures." The same may be said for pastoral areas in the east, where the area receiving enough rain to support pastoralism (250 mm per season) has been decreasing.

According to the Ministry of Water, Irrigation, and Energy (MoWIE, 2019), the total irrigated area in the Gidabo River watershed was 1,264ha, and recently expanding irrigation activities in the basin were reliant on available water supplies, which are being impacted by climate change. Limited studies have been undertaken in Gidabo with respect to the impact of climate change on runoff, according to revised literature in the research region (e.g. Degu A.M. et al., 2015; Shanka A.S., 2017), and they depended on single GCM or RCM, making their conclusions doubtful.

As a result, this research provides us with Current climate variability and catastrophic occurrences provide a significant basis for longer-term adaptation because it provides familiarity with climate and its socio-economic repercussions and consequences. Understanding how hydrological systems adapt to climate change and variability necessitates an understanding of how they are currently affected by those conditions as well as how they might behave in the future if those conditions change.

1.5. Scope of the Study

Results of this study will provide valuable information to water resources managers and policy makers in the Gidabo River Catchment. Moreover, application of up to date climate change scenarios will help to gain new insight about water resources problems and devising a compatible solution. However, it was not possible to cover the whole aspects of the study area with stated objective due to time and resource constraints. So it was better to limit the scope of the problem to a manageable objective.

Hence, this study utilized the time series of new probable climate scenario outputs of enhanced greenhouse gases for high emission scenarios (RCP 4.5 and 8.5) which are used as inputs for SWAT hydrologic model for the estimated runoff depth and peak discharge on the catchments in the basin. Though, the study addressed the impact of climate change on these global scenarios as inputs for hydrological model assuming that the land use land cover will remain the same. However, in real world land use/ land cover is always changing and it affects the hydrological responses in addition to emission of greenhouse gases.

2. LITERATURE REVIEW

2.1. Climate Change in Ethiopia and Gidabo River Catchment

Several studies have been carried out to estimate the influence of future climate change on Ethiopia's water resources at the water shade scale. Elsahmay et al. (2009), for example, used the Nile Forecasting Model with bias adjusted precipitation and temperatures from 17 GCMs to analyze the effects of climate change on the Blue Nile's stream flow. Ten of the 17 GCMs predict precipitation decreases, while seven predict precipitation increases. According to the findings, the future stream flow of the Blue Nile is highly unclear because to uncertainties in future precipitation change. Annual precipitation changes will range from -15 to +14 percent over the study area. Finally, they come to the conclusion that the annual total rainfall has remained relatively unchanged.

Bekele (2009) used one GCM (HadCM3 model) and two A2 and B2 emission scenarios to assess the impact of climate change on the Gilgel Abay reservoir. As a result, global temperatures are expected to rise by 0.6–1.4°C. For the A2a scenario, precipitation increases by 0.54 percent in the 2020s, 2050s, and 2080s, respectively, while for the B2a scenario, precipitation decreases by 0.54 percent in the 2020s, 2050s, and 2080s. For the A2 emission scenario, future river flow is expected to vary, with a drop of -3.73% in the 2020s and an increase in the 2050s and 2080s. According to the B2a emission scenario, annual inflow volume will fall by 2%%, 3% and 2.3% in 2020s, 2050s and 2080s respectively throughout all time horizons.

According to Abayneh (2011), using GCM model output, the research was able to evaluate the likely influence of climate change on extreme hydrological events and water availability in Addis Ababa and the adjacent catchment. Finally, the anticipated mean maximum and minimum temperatures for all months in both time periods (1930s and 1990s) demonstrate an upward tendency. In all time horizons, it is also predicted that there will be a substantial increase in flow volume in Bega season, up to 72 percent, and a declining increase in flow volume in Kermit season, up to 15 percent (1930s and 1990s).

Alemu's (2011) research on Addis Ababa, which used GCM outputs and HEC-HMS, showed that the maximum and minimum temperatures are expected to rise during the next 90 years.

The average monthly precipitation could rise or fall. In the 2030s, mean monthly precipitation might drop by up to 51%, whereas in the 2090s, it could rise by up to 131%. Climate change could result in a fall in monthly mean flow of up to 41% in the 2030s and an increase of up to 126% in the 2090s.

Also, according to Liben (2011), climate change has a substantial impact on the Upper Blue Nile Basin's water availability. The author claimed that the developed future scenarios for maximum and lowest temperatures typically show a rising trend, and a drop in precipitation is expected for the 2020s, 2050s, and 2060s, based on the outputs of RegCM3 (ECHAM5). In all time periods, Kiremt and Belge experienced increases in flow volume ranging from 48 percent to 185 percent and decreases range from 0.33 percent to 6.7 percent.

The research, by Zelalem, (2013), can be considered a recent study on climate change in the upper Blue Nile river basin. Using an analysis of previous climatic variability and future SRES A1B and A2 climate scenarios under three GCMs (ECHAM5, GFDL21, and CSIRO-MK3) climate models, the author attempted to evaluate the likely implications of climate change on hydrology and water resources. According to the findings, the mean maximum temperature will rise significantly for all future time periods. The findings of future stream flow simulations in the basin, utilizing both SDSM and LARS-WG downscaled output in SWAT, show a drop of 10% to -61% of the future Stream flow.

According to Nigatu et al. (2016), the prediction of mean annual over lake precipitation for both A2 and B2 emission scenarios reveals an increasing trend for the twenty-first century compared to the baseline period. For the three future eras, the increase in mean annual precipitation for the A2 emission scenario is 9% (112 mm/year), 10% (125 mm/year), and 11% (137 mm/year). Mean annual precipitation increases by 9% (111 mm/year), 10% (122 mm/year), and 10% (130 mm/year) for the three future periods under the B2 emission scenario. For both the A2 and B2 emission scenarios, the findings show constant increases in lake storage over the three future decades.

Shanka A.S., (2017) predicted that the total average annual runoff in the Gidabo river basin would increase by up to 3.4 percent, 2.9 percent, and 6.8 percent in the 2020s, 2050s, and 2080s for HadCM3 A2a and 5.1 percent, 5.6 percent, and 5.8 percent for HadCM3 B2a scenarios, respectively, in the 2020s, 2050s, and 2080s. In general, future average seasonal and annual runoff increased in all future time periods, with the exception of the Oct, Nov, Dec, and Jan month, as compared to the base period 1980-2000. During the summer season, there was a significant increase in average seasonal runoff, and during the Bega season, there was a significant decrease in magnitude.

Finally, Mamuye B. et al., (2017) reported that the minimum and maximum temperature trends in the Gidabo catchment of Ethiopia's Rift Valley Lakes Basin reached 0.08 °C/yr, with mean values indicating that the watershed was warming at 0.03 °C/yr to 0.07 °C/yr. The reported increase in temperature in the area has a substantial impact on agricultural activities, particularly in terms of soil water demand, as well as increased evapotranspiration, which causes the catchment to lose more water.

Variations in precipitation over monthly, seasonal, and annual time intervals influence hydrological variability in a Gidabo catchment. Variations in year-to-year variability in precipitation as well as changes in short-term rainfall attributes affect flood frequency in the catchment (such as storm rainfall intensity). As a result, most research used one or more GCMs, RCM outputs, and emission scenario(s), as well as direct GCM outputs or downscaled GCM outputs for driving a hydrological model. The outputs, on the other hand, are more varied and inconsistent, owing to the factors mentioned above.

One of the most significant obstacles to climate change in Ethiopia in general, and the Gidabo River Catchment in particular, is the scarcity of published material in the area. This demonstrates that, particularly in the Gidabo catchment, very little work has been done to measure or estimate the consequences of climate variability or extremes in detail. However, they concluded that there will be an increasing trend in maximum and lowest temperature in Ethiopia and the study area, as well as a slight change in precipitation, based on the examined literatures for the entire country and two literatures conducted in the study area.

Furthermore, Ethiopian climate change studies in water resources have mostly concentrated on existing information over the Blue Nile, with little research from the southern half of the nation, particularly the Gidabo river watershed.

2.2. Climate and Emissions Scenarios

Today, scenarios are vital for influencing climate change policy because they represent major driving forces, processes, impacts (physical, ecological, and economic), and potential solutions. In climate change research, various sorts of scenarios are significant within the overall category of scenarios. In analyzing climate change research, the IPCC has used emissions and climatic scenarios as a fundamental component.

Emissions Scenarios

"Emissions scenarios" are models that predict future releases of substances such as greenhouse gases and aerosols into the atmosphere that can affect the Earth's radiated balance, such as greenhouse gases and aerosols. Based on research into socioeconomic, environmental, and technological changes, integrated evaluation methods are used to make expert judgments about plausible future emissions. They are expert judgments about plausible future emissions based on research into socioeconomic and environmental trends represented in integrated assessment models as shown in Fig 2.1 (Richard H. et al., 2010).

"Short-term" fluctuations like business cycles or oil market price volatility are not taken into account when developing emissions scenarios for climate research. Rather, they concentrate on long-term (decades or centuries) energy and land-use trends. The gradual response of the climate system (centuries) to increasing greenhouse gas concentrations necessitates a long-term focus.

Climate Scenarios

Climate scenarios are plausible depictions of future climate conditions (temperature, precipitation and other climatological phenomena). Many different methods can be used to produce climate projections. These include: incremental techniques where climatic (or related) elements are increased by plausible amounts; spatial and temporal analogues that may resemble the future climate; extrapolation and expert judgment; and techniques that use a variety of methods (Mearns L.O. et al., 2001). There has been a noticeable uptick in interest in regional-scale climate scenarios and prediction methods, particularly for assessing impact and adaptation (Christensen J. H. et al., 2007).

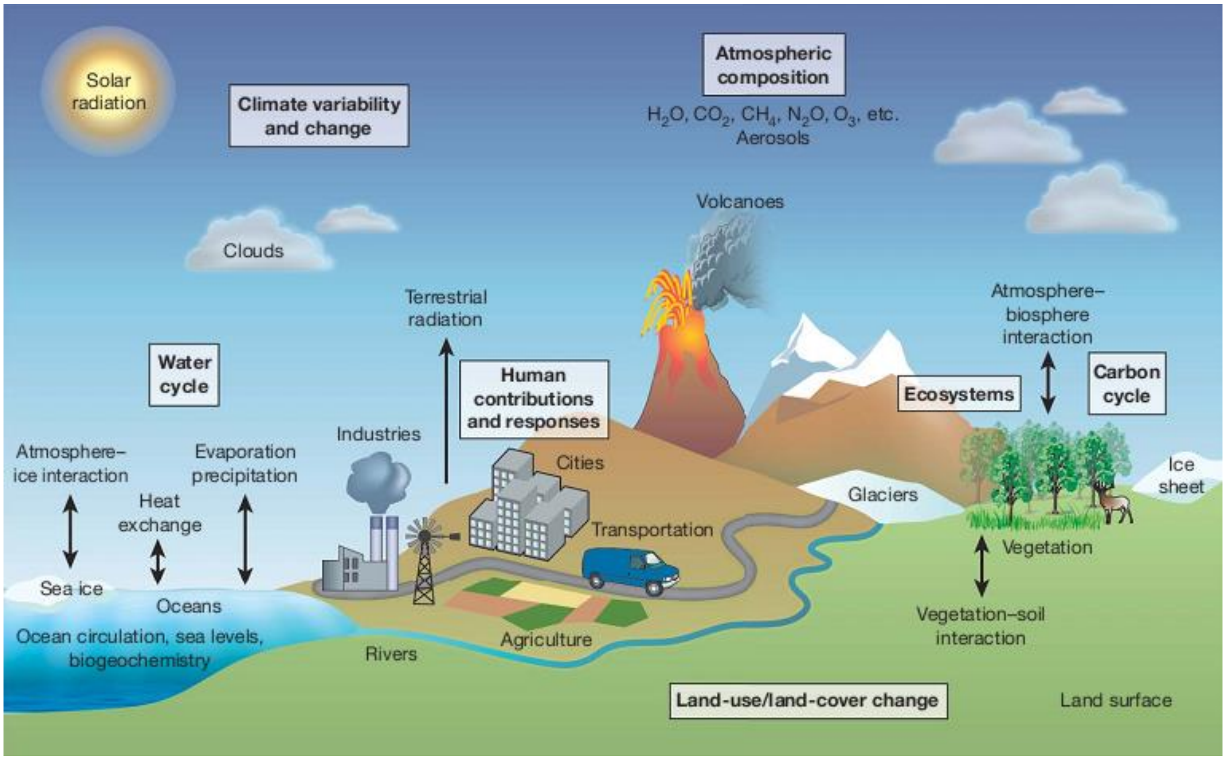

Figure 2.1: Major natural and anthropogenic processes and influences on the climate system addressed in scenarios (Richard H. et al., 2010).

2.2.1. Comparisons of SRES and RCPs Scenarios

Radiative forcing values for CMIP5 range from 2.6 to 8.5 W/m2 at 2100, a wider range than the three SRES scenarios used in CMIP3 (IPCC, 2013). Unlike the RCP scenarios, the SRES scenarios do not assume any policy to control climate change. At 2100, RCP4.5 and SRES B1 have similar radiative forcing, and their time evolution is comparable (within 0.2 W/m2) This is due to a faster decline in aerosol radiative forcing in RCP8.5 than in SRES A2, but the forcing do converge to within 0.1 W/m2 by 2100 (IPCC, 2013).

It falls somewhere between SRES B1 and SRES A1B, according to RCP6.0. The differences in temperature responses are consistent with differences in radiative forcing estimates, according to Dufresne et al., 2013 and Rogelj et al., 2012, as quoted on the IPCC, 2013. RCP2.6, which assumes strong mitigation action, results in a smaller temperature increase than any SRES scenario, according to a new study. There is little difference in the temperature increase between the RCP4.5 and SRES B1 scenarios. This is due to the wider range of radiative forcing across the RCP scenarios compared to the three SRES scenarios used in CMIP3.

2.2.2. RCPs Primary Characteristics and their Development

RCP 8.5: The International Institute for Applied Systems Analysis (IIASA), Austria, developed RCP 8.5 (High Emission) by combining the MESSAGE model with the IIASA Integrated Assessment Framework. This RCP is defined by growing greenhouse gas emissions over time, which is typical of literature scenarios that result in high greenhouse gas concentration levels (Riahi et al., 2007).

RCP 6: The AIM modeling team of Japan's National Institute for Environmental Studies (NIES) generated RCP6. It is a stabilization scenario in which total radiative forcing is stabilized shortly after 2100, with no overshoot, using a variety of technologies and tactics to reduce greenhouse gas emissions (Fujino et al., 2006; Hijioka et al., 2008).

RCP 4.5: The GCAM modeling team at the Joint Global Change Research Institute (JGCRI) at the Pacific Northwest National Laboratory in the United States developed RCP 4.5. It's a stabilization scenario in which total radiative forcing stabilizes shortly after 2100 without exceeding the long-term radiative forcing target level (Clarke et al., 2007; Smith and Wigley, 2006; Wise et al., 2009).

RCP2.6: The PBL Netherlands Environmental Assessment Agency's IMAGE modeling team came up with RCP2.6. The emission pathway is based on published scenarios that result in extremely low greenhouse gas concentrations. It's a "peak-and-decline" scenario, in which radiative forcing rises to roughly 3.1 W/m2 by mid-century and then falls to around 2.6 W/m2 by 2100. To achieve such levels of radiative forcing, greenhouse gas emissions (and consequently air pollution emissions) must be significantly lowered over time (Van Vuuren et al., 2007a; Characteristics quoted from van Vuuren et al., 2011).

2.3. Climate Models

Climate models are mathematical representations of processes that affect the Earth’s climate. This study will analyze the results of a hierarchy of climate models, ranging from simple idealized models through intermediately complicated models to comprehensive General Circulation Models (GCMs) and Regional Climate Models (RCMs).

2.3.1. Global Climate Models

Global Climate models (GCM) are designed to simulate the earth's climate over the entire planet; it has limitations when it comes to describing local details of climate features owing to their coarse spatial resolution. The coarse resolution prohibits global models from providing an accurate description of extreme events with respect to the regional and local impacts of climate variability and change (Giorgio et al., 2009). Hence, downscaling of the climate from the coarse resolution GCMs to regional scale for the computation of the local details to obtain the relevant temporal and spatial scales pertinent for climate change studies is required.

2.3.2. Regional Climate Models

RCMs dynamically downscale GCM output to sizes more suitable to end-users, and are valuable for understanding local climates in places with complicated terrains, such as eastern Africa (Endris et al., 2013). The number of RCM simulations has increased dramatically globally (Alley et al., 2007); however, only a few RCM investigations have been conducted over the East African region (Anyah and Semazzi, 2007; Segele et al., 2009a, and Diro et al., 2012), and these studies are primarily based on the findings of four RCM. Each model, though, has its own set of advantages and disadvantages.

As a result, a collection of RCMs must be used, however, this has never been done before due to a lack of a large ensemble of RCM output that accounts for land surface heterogeneity (Gbobaniyi et al., 2014). RCMs also serve as a zooming mechanism for delivering climatic data from a regional to a local scale (Akinsanola and Ogunjobi, 2017).

2.3.3. Coordinated Regional Climate Downscaling Experiment

The Coordinated Regional Climate Downscaling Experiment (CORDEX) is a worldwide initiative to help climate change impact and adaptation research by making fine-scale climate predictions (about 50 km) freely available to users. Downscaling is done using an RCM with starting and boundary conditions derived from chosen GCMs or reanalysis data (a combination of climate model and observable data) (Haile A.T. et al., 2015). Currently, the World Climate Research Program's CORDEX program allows for the generation of high-resolution regional climate predictions that may be used to estimate future climate change consequences at regional scales (Giorgi et al., 2009).

Endris et al., (2013) found that the simulation results of 10 CORDEX-Africa models captured the form of the monthly rainfall distribution and the annual rainfall anomaly for the Ethiopian highlands, but underestimated the mean monthly rainfall quantity. The study found that for four RCMs, the correlation coefficient between yearly rainfall and the reference data set is greater than 0.7, and for six models, it is between 0.4 and 0.7. It was shown that the multimodal ensemble mean accurately mimics eastern Africa rainfall and can thus be used to evaluate future climate forecasts for the region.

The major driver of Kiremt-season precipitation is thermal forcing on-air parcels along with southwesterly flows (Segele and Lamb, 2005). The resolution of these key topographical features, which encompass an 8° region, necessitates the use of at least 16 model grids (Pielke, 2002). Thus, for GCMs to model the influence of topography on Ethiopian precipitation, a horizontal resolution of 2° is required (Pielke, 2002 and Feser et al., 2011). They divided the 30 CMIP5 models into two categories using a 2° horizontal-resolution cut-off: high-resolution models and low-resolution models.

When comparing the two groups, the high-resolution models perform better at reproducing area-averaged precipitation than the low-resolution models. The ensemble of high-resolution models, in particular, suggests an average precipitation rate of 3.69 mm/day for Ethiopia, which is quite comparable to observations. The precipitation rate in the ensemble of low-resolution models, on the other hand, is 2.6 mm/day, which is about 30% lower than actual precipitation (Li et al., 2015). As a result, it is preferable to employ the top-rated (at least top 4) high-resolution RCM or GCM ensembles when utilizing CORDEX.

2.4. Hydrological Modeling

Hydrological models are mathematical formulations which determine the runoff signal which leaves a watershed basin from the rainfall signal received by this basin. They provide a means of quantitative prediction of catchment runoff that may be required for efficient management of water resources. Such hydrological models are also used as means of extrapolating from those available measurements in both space and time into the future to assess the likely impact of future hydrological change.

The catchment hydrological model is a collection of mathematical description of components of the hydrologic cycle. Hydrological models are the main tools for hydrologists for purpose of water resource management, planning and development, assessing effect of land use change, flood prediction, water quality assessment etc. (Jajarmizadeh et al., 2012). In addition to assess the most likely hydrological impact of future hydrological system responses, for example to climate and land management change.

Depend on the problem that needs to be addressed hydrological model applications have many objectives. These are:

1. Long term prediction of hydrological parameters, for the given climate and hydrological conditions by extrapolation of point measurements in both space (for un-gauged sites, sub basin etc.) and time (Pechlivanidis et al., 2011), and also for expected changes in land use and other scenario (Nemec, 1993), and
2. Planning and design of hydraulic structures for water supply, waste water treatment, flood control and protection etc.

2.4.1. Hydrological Modeling in Climate Change Studies

Hydrological models are mathematical formulations that determine the runoff signal, which leaves a watershed basin from the rainfall signal received by this basin. They provide a means of quantitative prediction of catchment runoff that may be required for efficient management of water resources. Such hydrological models are also used as means of extrapolating from those available measurements in both space and time into the future to assess the likely impact of future hydrological change.

Changes in global climate are believed to have significant impacts on local hydrological regimes, such as in stream flows which support aquatic ecosystem, navigation, hydropower, irrigation system, etc. In addition to the possible changes in total volume of flow, there may also be significant changes in frequency and severity of floods and droughts. Hence, hydrological models provide a framework to conceptualize and investigate the relationship between climate and water resource.

Chong-vu Xu mention the advantages of hydrological models in climate change impact studies as follows (Xu, 1999):

1. Models tested for different climatic/physiographic conditions, as well as models structured for use at various spatial scales and dominant process representations, are readily available.
2. GCM-derived climate perturbations (at different level of downscaling) can be used as model input.
3. A variety of response to climate change scenarios can be modeled.
4. The models can convert climate change output to relevant water resource variables related, for example, to reservoir operation, irrigation demand, drinking and water supply.

2.4.2. Selection of Model

The choice of the best model depends on the problem. Model must be evaluated and selected before applied to estimate catchment output. The selection of hydrological model should include structure of the model, time step, representation of physical process, requirement on input data and hardware/software (Nemec, 1993).

Nowadays, there are different models used to predict the hydrology of a given watershed and also developed partly to quantify the influence of change in land use, land cover and management practices on the hydrologic cycle. MIKE SHE (Butts et al., 2005), SWAT (Arnold et al, 1998), HEC-HMS (Choudhari et al, 2014), HBV (Bergstrom, 1992) are some of the models.

The boundary conditions for selecting the right model to fulfill the objectives of the study are listed as follow:

- Generally model selection is based on desktop review and evaluation of selected models (Nemec, 1993).(there is no testing of the model)
- The model output must be important to the study (It should be able to simulate the stream flow and sediment yield)
- The minimum input data requirements for the model must be available or can be estimated with some methods using data from the watershed.
- Its time scale should be long term, continuous and able to simulate on daily bases for water budget analyses at watershed and sub-watershed levels (Kassa, 2009), because

event models have no provision for moisture recovery between storm events (Asmamaw, 2013)

- The model must be readily and freely available, both for research and for future use in Ethiopia.
- The ability of a hydrological model to integrate GIS for hydrologic data development, spatial model layers and interface (Kassa, 2009).

Generally for this study, a semi-distributed model is best fit because of the model structure is more physically-based than the structure of lumped model, and the model is less demanding on input data than fully distributed model (Jajarmizadeh et al., 2012), Based on the model selection guideline described above the SWAT hydrological model is selected among the models and reviewed in detail.

2.4.3. Soil and Water Assessment Tool

Soil and Water Assessment Tool (SWAT) is a river basin, or watershed scale model developed to predict the impact of land management practices on water, sediment, and agricultural chemical yields in large, complex watersheds with varying soils, land use, and management conditions over long periods of time. The model breaks the entire catchment in to sub catchments which are further divided in to hydrologic response units (HRU) based on land use, vegetation and soil characteristics.

The model combines empirical and physically-based equations, uses readily available inputs, and enables users to study long-term impacts (Winchell et al., 2013). It simulates eight major components: hydrology, weather, sedimentation, soil temperature, crop growth, nutrients, pesticides, and agricultural management (Neitsch et al., 2011). Major hydrologic processes that can be simulated by the model include evapo-transpiration, surface runoff, infiltration, percolation, shallow aquifer and deep aquifer flow, and channel routing. The simulation of the processes can be done in four subsystems: surface soil, intermediate zone, shallow and deep aquifers, and open channels. Stream flow in a main channel is determined by three sources: surface runoff, lateral flow and base-flow from shallow aquifers.

The model has been applied to predict stream flow and it shows good agreement with measured data for different types of watershed (Khalid et al., 2016; Kim and Pachepsky, 2010;

Singh et al., 2013), and SWAT was also applied to predict various impacts of land management and climate change on water quantity, sediment yield and soil erosion (Asselman et al., 2003 and Zheng et al., 2016).

SWAT is also applied in Ethiopia to model the hydrological process, sediment yield and estimate water balance (Abraham et al., 2015; Asmamaw, 2013; Fasil, 2012, and Kassa, 2009). The overall performance of the model in most cases is acceptable.

3. MATERIAL AND METHODS

3.1. Study Area Description

The Gidabo River is a medium-sized perennial river of south-central Ethiopia within the Great Rift Valley. The Gidabo River catchment area is one of the leading coffee production areas in Ethiopia. It is one of three medium-sized rivers discharging into Lake Abaya. The roughly 120 km long river rises on the western slopes of the Soka Sonicha mountain range (with the most prominent being the Gelala mountain) at 6.8°N 38.6°E, flows west first and then for most of its course southwards along the eastern floor of the Great Rift Valley and through the Sidama Zone. It passes the notable town of Yirgalem. The location map of the Gidabo River Catchment is presented in Figure 3.1.

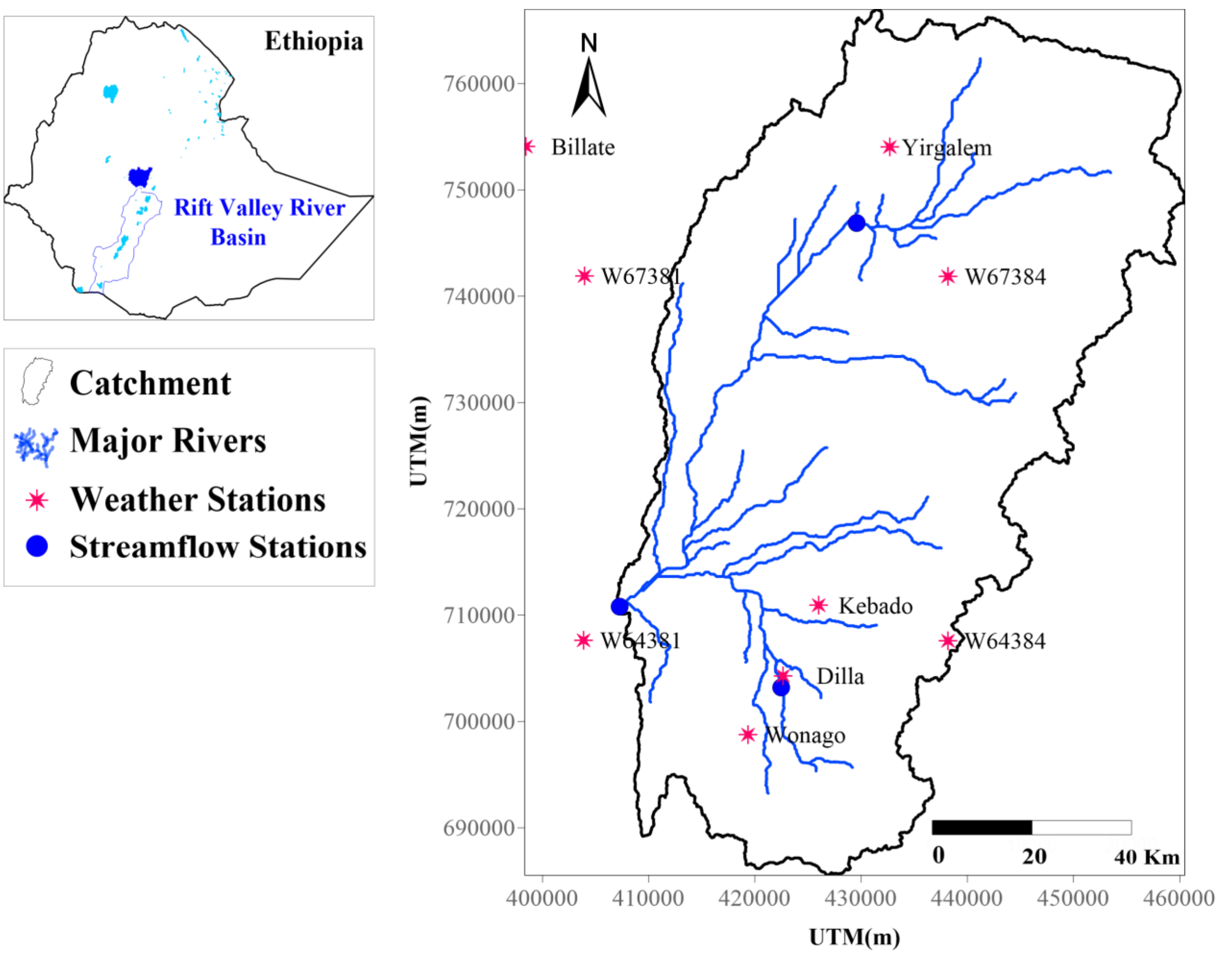

Figure 3.1: Location map of the Gidabo River Catchment

The river turns westward when entering the Gidabo flood plains directly east of Lake Abaya. It finally drains into Lake Abaya at 6.56°N 38.05°E. In the flood plains and along the final stretch of the river it defines the southern border of the Sidama Zone through which it flows for most of its length. The town of Dilla is the most prominent town in the catchment area of the river. Another town in the catchment area is Aletawendo.

3.2. Data Availability

3.2.1. Meteorological Data

Meteorological data was used as input to the SWAT model in hydrological model development. The meteorological data was collected during the field survey from the Ethiopian National Meteorological Agency in Addis Ababa. Since there are few meteorological stations which have relatively long period of record inside the catchment, data was also collected from the station surrounding the catchment as shown in the table 3.1.

Table 3.1: List of station name, location and topography

ID	NAME	LAT	LONG	ELEVATION
1	Billate	6.82	38.08	1361
2	Dilla	6.37	38.3	1579
3	Kebado	6.43	38.33	1807
4	Wonago	6.32	38.27	1748
5	Yirgalem	6.82	38.39	1786
6	W64381	6.4	38.13	1198
7	W67381	6.71	38.13	1438
8	W64384	6.4	38.44	2734
9	W67384	6.71	38.44	1829

3.2.2. Hydrological Data

The stream flow of Gidabo River basin was required for calibrating and validating the model. There are three main gauging stations (Aposto, Meassa and Beddasa) inside the catchment which have continuous record for a relatively long period and therefore daily stream flow data (1998- 2010) for these stations were collected during the field work from the Hydrology Department of Ministry of Water resources.

3.2.3. Climate Scenario Data

Climate scenario data is required to quantify the relative change of climatic variables between the current and future time horizon which in turn is used as input to hydrological model for assessment of hydrological impacts. The CORDEX program archives outputs from a set of RCM simulations over different regions in the world. The CORDEX domains for model integrations are found at (http://wcrp-cordex.ipsl.jussieu.fr/images/pdf/cordex_regions.pdf) for the RCP 4.5 and RCP 8.5 projection scenario.

In this study datasets from CORDEX Africa are accessed from (http://cordexesg.dmi.dk/esgf-web-fe). The datasets are quality controlled and may be used according to the terms of use (http://wcrp-cordex.ipsl.jussieu.fr).

The spatial grid resolutions of all CORDEX Africa RCMs were set to longitude 0.44° and latitude 0.44° using a rotated pole system coordinate. These models operate over an equatorial domain with a quasi-uniform resolution of approximately 50 km by 50 km. For detailed description of CORDEX RCMs and their dynamics and physical parameterization consult Nikuli et al. (2012). In this study outputs of ICHEC EC-EARTH GCMs were used and the outputs used were dynamically downscaled CCLM4, RCA4, RACMO22T, and REMO2009 regional climate models.

Table 3.2: Description of Regional Climate Models considered in this study

RCM	Full Name	Institute	Reference
CCLM	CLMcom COSMO-CLM version 4.8	Climate Limited-Area Modeling (CLM) community	Baldauf et al. (2011)
RCA4	SMHI Rosby Center Regional Atmospheric Model (RCA4)	Sveriges meteorologiska och institut (SMHI), Sweden	Samuelsson et al. (2011)
REMO	MPI regional model (REMO)	Max Plank Institute (MPI), Germany	Jacob et al. (2007)
RACMO22T	KNMI Regional Atmospheric Climate Model, version 2.2	Koninklijk Nederlands Meteorologisch Instituut (KNMI), Netherlands	Obed M.O. et al., (2020)

3.2.4. Data Processing and Analysis

In order to construct detailed climate change scenarios for the Gidabo River catchment and assess their impacts on water availability, a SWAT hydrological model was used. As the result of any simulation depends of the quality of the available data, data checking were made for their reliability.

As the reader most probably knows, meteorological stations are not only recording the local climate variations, but rather their measurements are also affected by changes in instrumentation, methods of observation, relocations and changes in the environment (e.g. urban growth or land use changes). This introduces in homogeneities in the observational series, and we call homogenization the process that tries to remove this unwanted perturbation and let the climatological series to reveal only the climate variations.

Some old methods relayed on tests to check the non-stationary of a single climatological series. This absolute method must be avoided, since they assume a climate stability that has proved unrealistic. The alternative was to use relative homogenization methods, in which the stationary test were applied to series of ratios or differences between the problem station and one or more well correlated series from neighbor stations (Jose A.G, 2018).

In this study The "Climatol" R contributed package was used to the problem of homogenizing climatological series; that was to say, remove the perturbations produced by changes in the conditions of observation or in the nearby environment to allow the series to reflect only (as far as possible) the climatic variations. In its beginnings, this program was focused on infilling the missing data by estimates calculated from the closest series. This was done by adapting the method from Paulhus and Kohler (1952) to infill daily rainfall data by averaging neighboring values, normalized by dividing them by their respective average rainfall.

This method was chosen for its simplicity and for allowing the use of nearby series even if they did not have a common period of observation with the problem series, which would preclude the adjustment of regression models. In addition to normalizing the data through a division by their average values, Climatol also offers the possibility of subtracting the means or applying a full standardization. So, letting m_x and S_x be the average and standard deviation of a X series, we have these options for their normalization:

1. Remove the mean: $x = X - m_X$ *(3.1)*

2. Divide by the mean: $x = X / m_X$ *(3.2)*

3. Standardize: $x = (X - m_X) / s_X$ *(3.3)*

The main problem with this methodology is that means (and standard deviations in the third case) of the series in the study period are unknown when the series are not complete, which is most often the case in real data bases. Then Climatol first calculates these parameters with the available data in each series, infill the missing data using these provisional averages and standard deviations, and recalculates them with the in filled series. Then data the originally missing data are recalculated using the new parameters, which will lead to new means and standard deviations, hence repeating the process until no average changes when rounded up to the initial precision of the data. The flow chart of the *climatol* operation is shown in Fig 3.2.

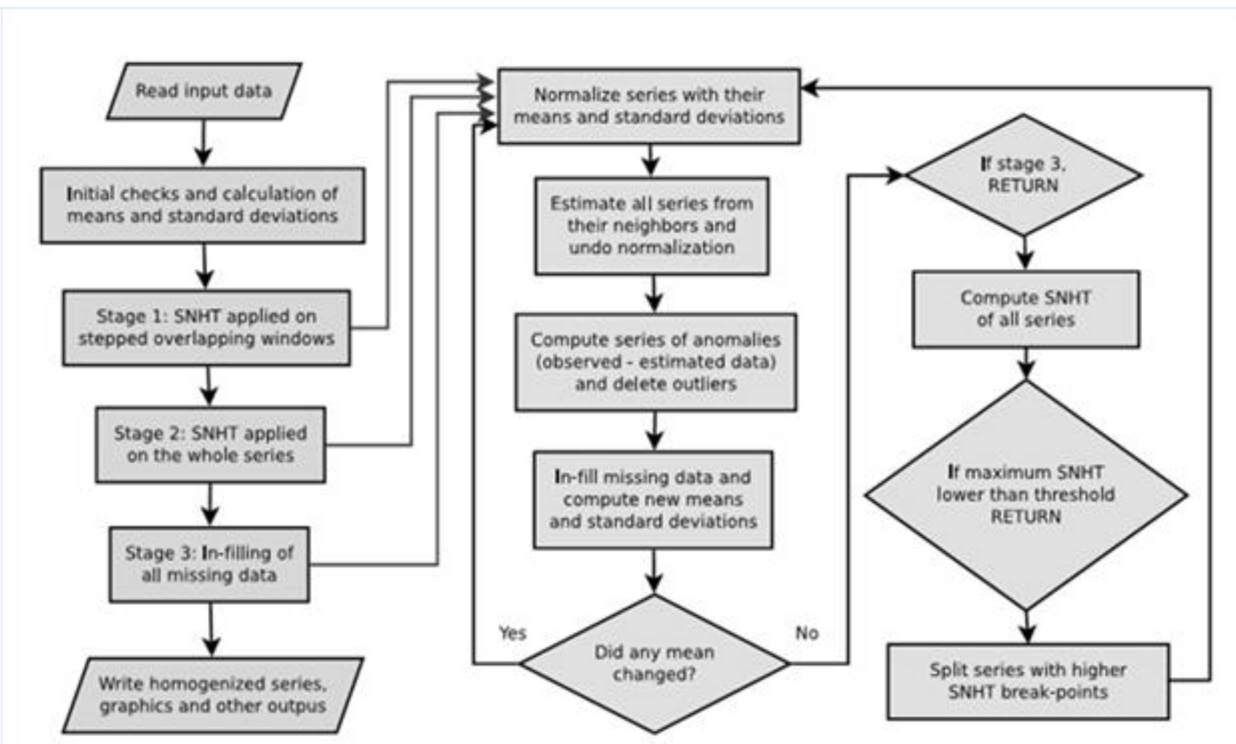

Figure 3.2: Flow chart of the climatol operation, showing its nested iterative processes (Jose A.G., 2018).

3.3. Correction of Biased RCM Simulations

CMhyd was used to provide simulated climate data that can be considered representative for the location of the gauges used in a watershed model setup. Therefore, climate model data should be extracted and bias-corrected for each of the gauge locations.

Purpose of Bias Correction

Bias correction procedures employ a transformation algorithm for adjusting RCM output. The underlying idea is the identification of possible biases between observed and simulated climate variables, which is the basis for correcting both control and scenario RCM runs. Bias correction methods are assumed to be stationary, i.e., the correction algorithm and its parameterization for current climate conditions are also valid for future conditions. The following bias correction methods were used to adjust RCM simulations: (1) power transformation, (2) variance scaling.

3.3.1. Power Transformation for Precipitation

The precipitation is usually varied spatially and highly nonlinear in nature. Power transformation is a nonlinear method which corrects both mean and variance of precipitation (Yang, *et al*., 2015). In this study the RCM data of precipitation was bias corrected by using Power Transformation Method because it corrects the mean, variance and coefficient of variation (CV), leads to a better copy of observed precipitation. The correction method is applied by comparing the daily observed precipitation at each station with the nearest grid point of the RCM considering the grid points as a single station on the watershed.

3.3.2. Variance Scaling for Temperature

The PT method is an effective method to correct both the mean and variance of precipitation, but it cannot be used to correct temperature time series, as temperature is known to be approximately normally distributed (Yang et al., 2015). The VARI method was developed to correct both the mean and variance of normally distributed variables such as temperature (Teutschbein and Seibert, 2012). The bias correction framework is shown in Figure 3.3.

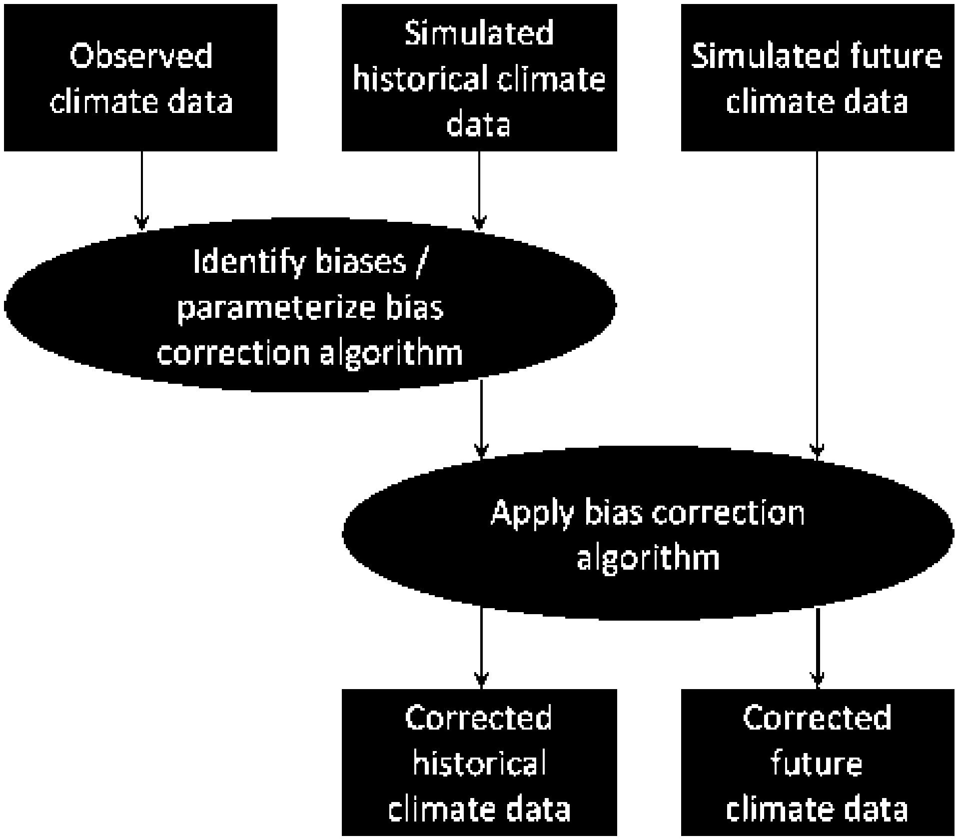

Figure 3.3: Bias Correction Framework (Rathjens et al., 2016)

3.4. Mann Kendall Trend Test

Mann-Kendall (Mann, 1945; Kendall, 1975) rank-based non-parametric statistical tests applied in many hydro-climatological studies, which used for detecting monotonic trends in time series data. Yue and Wang (2002) indicated that the power of the trend depends on the pre assigned significance level, magnitude of trend, sample size, and the amount of variation within a time series. That is, the bigger the absolute magnitude of trend, the more powerful the tests are; as the sample size increases, the tests become more powerful (Sen, 2012).

The presence of significant trends in the variables using Mann Kendal test is more applicable and employed by many researchers. The test is advantageous over parametric tests because of that the test does not require the data to be normally distributed. It is distribution free, more robust and tolerates missing values and outliers. The test is also rank based analysis in time series (Burn et al., 2004 and Tesemma et al., 2010).

The Mann-Kendal trend test was used in this study to investigate trends in the climatic and stream flow variables considered. The test was based on S statistics and each paired observed values Xj (j > k) of the random variable were inspected to find out whether Xj > x_k or Xj < Xk.

Error! Reference source not found.Error! Reference source not found.Error! Reference source not found. *(3.4)*

Where X_j and X_k are the annual data values in years j and k, j > k respectively and n is number of observation.

Error! Reference source not found.Error! Reference source not found.

(3.5)

S is normally distributed with mean 0, and Variance,

Error! Reference source not found.

(3.6)

The variance VAR(S) and Z are computed using equations (3.5) and (3.6) and respectively.

Computation for Z score is obtained as:

Error! Reference source not found.

(3.7)

For a given level of significance *a*, the null hypothesis of no trend in the time series will be rejected if \Z\ > $z_{1—\alpha}$. More specifically, Z > $Z_{1-\alpha}$ indicates existence of an increasing trend and Z < Z_α implies a decreasing trend.

The test statistics Z was used as a measure of significance of trend. If the value of Z is positive, it indicates increasing trends, while negative values of Z show decreasing trends. If |ZS| is greater than Zɑ/2, where ɑ the chosen significant level (5% with Z 0.025= 1.96) then the null hypothesis is invalid implying that the trend is significant (Modarres and da Silva, 2007).

3.5. SWAT Hydrological Model

SWAT is semi-distributed, physically based, continuous time, a widely used and flexible modeling tool, which addresses many aspects of catchment (Thomas et al., 2015). One of the main advantages of SWAT is it can be used to model watersheds with less monitoring data (Asmamaw, 2013; Abraham et al., 2015). SWAT model has gained international acceptance as inter disciplinary watershed modeling tools by many international SWAT conferences (Gassman, 2007), can be downloaded freely from http://swat.tamu.edu/software. The interface of SWAT model is compatible with ArcGIS that can integrate many available geospatial data to accurately represent the characteristics of the watershed (Asmamaw, 2013).

Weather variables for computing the hydrologic balance in SWAT are precipitation, air temperature, solar radiation, wind speed and relative humidity, daily inputs can be entered directly or the weather generator can be used to simulate daily values for these variables (Weather generator can be download from the SWAT web (site http://swat.tamu.edu/software) other than these DEM (Digital Elevation Model), soil map, land use map also needed for the model.

Simulation of the hydrology of a watershed can be separated into two major parts. The first part is the land phase of the hydrologic cycle. The land phase of the hydrologic cycle controls the amount of water, sediment, nutrient and pesticide loadings to the main channel in each sub basin. The second division is routing phase of the hydrologic cycle which can be defined as the movement of water, sediments, nutrient etc…, through the channel network of the watershed to the Outlet.

3.5.1. Hydrological Component of SWAT

The Simulation of the hydrology of a watershed was done in two separate divisions. One was the land phase of the hydrological cycle that controls the amount of water, sediment, nutrient and pesticide loadings to the main channel in each sub-basin. The second division was routing phase of the hydrologic cycle that can be defined as the movement of water, sediments, nutrients and organic chemicals through the channel network of the watershed to the outlet. In the land phase of hydrological cycle, SWAT simulates the hydrological cycle based on the water balance equation.

Error! Reference source not found. *(3.8)*

Where: SW_t is the final soil water content (mm), SW_o is the initial soil water content on day i (mm), t is the time (days), R_{day} is the amount of precipitation on day i (mm), Q_{surf} is the amount of surface runoff on day i (mm), Ea is the amount of evapotranspiration on day i (mm), Wseep is the amount of water entering the vadose zone from the soil profile on day i (mm), and Qgw is the amount of return flow on day i (mm).

Land phase of the hydrological cycle: The main hydrological components simulated in the land phase of the hydrological cycle are evapotranspiration, lateral subsurface flow, groundwater flow, surface runoff, ponds, canopy storage, infiltration, redistribution, tributary channels, and return flow. SWAT simulates the land phase of the hydrological cycle based on the water balance equation.

Routing phase of the hydrologic cycle: The second phase of the SWAT hydrologic simulation, the routing phase, consists of the movement of water, sediment and other constituents (e.g. nutrients, pesticides) in the stream network. The change in channel dimensions with time due to down cutting and widening is also included. Similar to the case for the overland flow, the rate and velocity of flow is calculated by using the manning's equation.

Percolation is the downward movement of water in the soil. SWAT calculates percolation for each soil layer in the profile. Water is allowed to percolate if only the water content exceeds the field capacity of that layer (Neitsch et al., 2002).

Surface runoff occurs whenever the rate of precipitation exceeds the rate of infiltration. SWAT offers two methods for estimating surface runoff: the SCS curve number procedure and the Green and Ampt infiltration method. Using daily or sub daily rainfall, SWAT simulates surface runoff volumes and peak runoff rates for each HRU. The SCS curve number method was used to estimate surface runoff because of the unavailability of sub daily data for Green and Ampt method.

Lateral flow is common in areas with high hydraulic conductivities in surface layers and an impermeable or semi-permeable layer at a shallow depth. Rainfall will percolate vertically up to the impermeable layer and develops a saturated zone stored above this layer. This is called a perched water table, which is the source of water for lateral subsurface flow. SWAT incorporates a kinematic storage model for subsurface flow (Neitsch et al., 2002).

Peak discharge or the peak surface runoff rate is the maximum volume flow rate passing a particular location during a storm event. SWAT calculates the peak runoff rate with a modified rational method. In rational method it is assumed that a rainfall of intensity i begins at time t = 0 and continues indefinitely, the rate of runoff will increase until the time of concentration, t = tconc. The modified rational method is mathematically expressed as:

Error! Reference source not found. *(3.9)*

Where: q_{peak} is the peak runoff rate (m3/s), αtc is the fraction of daily rainfall that occurs During the time of concentration, Q_{surf} is the surface runoff (mm), Area is the sub-basin area (km^2), tconc is the time of concentration (hr), and 3.6 is a conversion factor.

Potential evapo-transpiration: there are many methods that are developed to estimate potential evapo-transpiration (PET). Three methods are incorporated into SWAT: the Penman-Monteith method, the Priestley-Taylor method, and the Hargreaves method. In this study potential evapotranspiration is calculated with the Hargreaves 'approach due to missing or unavailability of weather data for the stations used. For stations with only temperature but no other variables required by Hargreaves method was used to calculate potential evapo-transpiration. Hargreaves derived an equation to calculate potential evapo-transpiration using only temperature, which is a measurement that can be made most accurately, and extraterrestrial radiation Ra using the relation:

Error! Reference source not found. *(3.10)*

Where: PET_{HG} is the potential evapo-transpiration by the Hargreaves method (mm/day), Ra is the extra-terrestrial radiation (mm/day); T_{mean} is the average temperature (°C); Tmax and Tmin are the maximum and minimum temperature (°C), respectively.

Groundwater: the simulation of groundwater was partitioned into two aquifer systems i.e. an unconfined aquifer (shallow) and a deep-confined aquifer in each sub basin. The unconfined aquifer contributes to flow in the main channel or reach of the sub basin. Water that enters the deep aquifer is assumed to contribute to stream flow outside the watershed (Arnold et al., 1993). The water balance for a shallow aquifer is calculated with equation 2.4.

Error! Reference source not found. *(3.11)*

Where: aqsh, i is the amount of water stored in the shallow aquifer on day i (mm), aqsh,i-1 is the amount of water stored in the shallow aquifer on day i-1 (mm), Wrchrg is the amount of recharge entering the aquifer on day i (mm), Qgw is the groundwater flow, or base flow, into the main channel on day i (mm), WRevap is the amount of water moving into the soil zone in response to water deficiencies on day i (mm), Wdeep is the amount of water percolating from the shallow aquifer into the deep aquifer on day i (mm), and Wpump, sh is the amount of water removed from the shallow aquifer by pumping on day i (mm).

3.5.2. Model Input Data

SWAT model requires two kinds of data; these are spatial data and temporal data. Spatial data include a digital elevation model (DEM), land-use map and soil map. The temporary data include hydrological data (stream flow & sediment yield) and climatic data (precipitation, solar radiation, relative humidity, wind speed and temperature). These data were collected from different sources and databases.

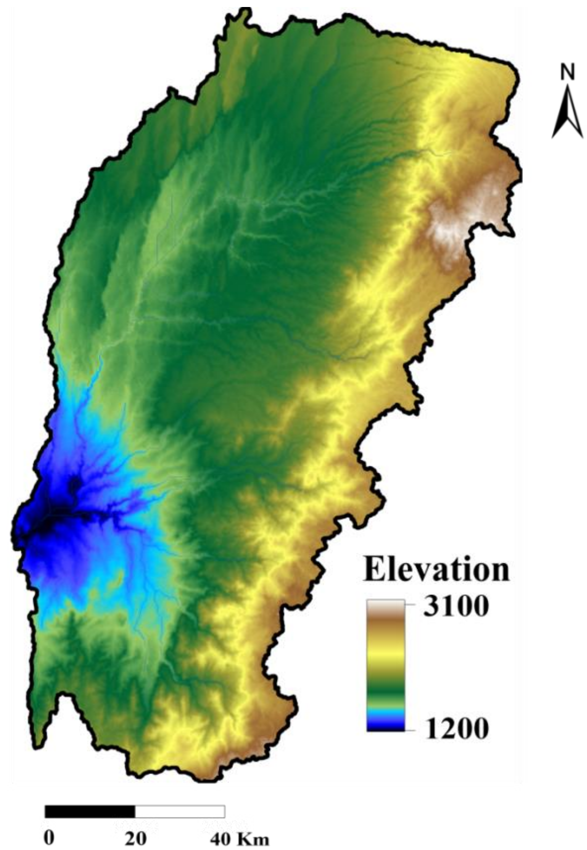

Figure 3.4: DEM of Gidabo River Catchment

Digital Elevation Model

Digital Elevation Model (DEM) data is required to calculate the flow accumulation, stream networks, and watershed delineation using SWAT watershed delineator tools. A 30m by 30m resolution Digital Elevation Model was obtained from Ministry of Water Irrigation Energy and Electricity Addis Ababa, Ethiopia. This data was projected to Universal Transverse Mercator zone 37^0N on spheroid of WGS_1984 and it was in raster format to fit in to the model requirement (see Figure.3.4).

Weather Data

SWAT requires daily meteorological data that can be read from a measured data or can be generated by a weather generator model. In this study, the weather variables used for driving the hydrological balance are daily precipitation, minimum and maximum air temperature, relative humidity, wind speed, and daily sunshine hours for the period 1995–2010. These data were obtained from Ethiopian National Meteorological Agency (NMA) for stations located in and around the watershed (See Figure.3.1). Using the selected data quality assessment method the weather stations selected for this study out of 13 stations are nine stations the rest stations excluded because they failed in the testing process. Missing values were identified in some of the climatic variables. These values were assigned with no data code (-99) which then filled by the weather generator in the SWAT model from monthly weather generator parameters values. The monthly generator parameter values were estimated from Billate and Dilla stations.

Soil Data

Soil map of the Gidabo River Catchment is obtained from MoWIE. Soil is an important factor in determining the amount of run-off in a catchment. Different soil properties in a catchment can have a major effect on the rate of the lags in hydrological processes (Perry, 2015). In addition to soil map soil physical and chemical properties such as soil texture, available water content, hydraulic conductivity, bulk density and organic carbon content for different layers of each soil type where obtained from Harmonized World Soil Database v 1.2 see Appendix VI. The soil texture map of the study area is shown in Figure.3.5.

To combine the soil map with SWAT model, a user soil database which contains textural and chemical properties of soils was prepared for each soil layers and added to the SWAT user soil databases. The lookup table was also prepared to connect soil map to SWAT user soil databases in the GIS interfaces using name option. Areal coverage of the soil types are presented in Table 3.3.

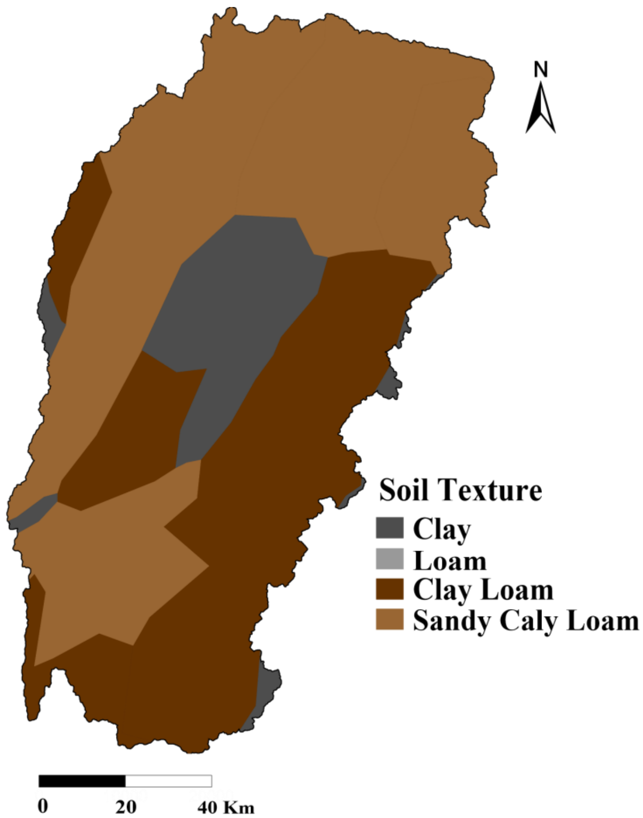

Figure 3.5: Soil map of Gidabo River Catchment

Table 3.3: Soil types of Gidabo River Catchment and their areal coverage

Soil Types	Area	
	Km^2	%
Clay	575.33	21.83
Loam	84.88	3.22
Clay Loam	887.13	33.66
Sandy Clay Loam	1088.42	41.29
Total	2635.76	100.00

The soil map of the study area was prepared in raster format to fit the model requirement and was given to the model. The user soil database was linked to soil map using the look up table, which was given as input to the SWAT model in .dbf (data base) format.

Land Use and Land Cover

The hydrological properties of the watersheds are highly influenced by Land use. It is one of the main input data of the SWAT model to describe the Hydrological Response Units (HRUs) of the watersheds (Kassa, 2009). The information contained in the land use/land cover shows how the different uses of the surface are distributed inside the study area. For this study the land uses/cover were obtained for the year 2000 from GlobeLand30. The 2000 land use/land cover map of Gidabo River Catchment used for model setup is shown in Figure 3.6.

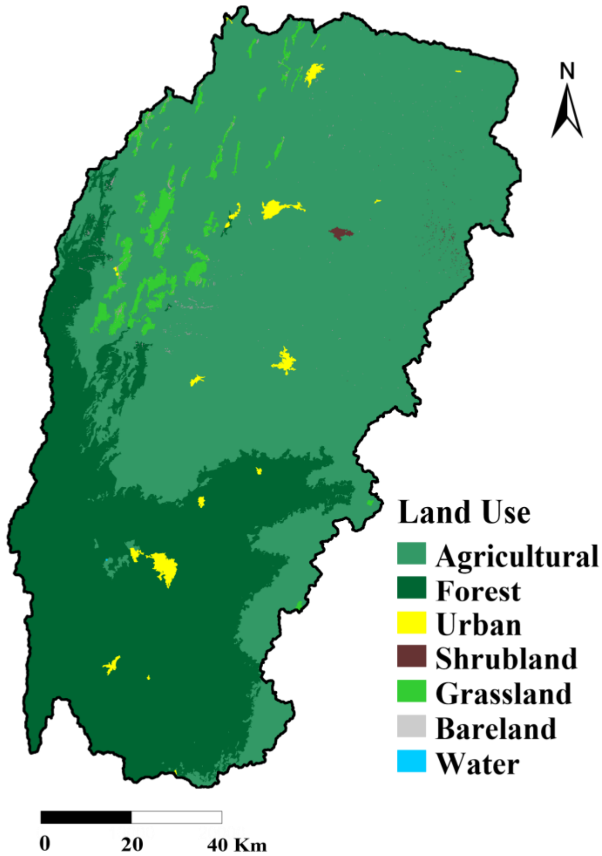

Figure 3.6: Land use/land cover map of Gidabo River Catchment in year 2000

SWAT has predefined land uses identified by four letter codes and it uses these codes to connect land use to SWAT land use databases in the GIS interfaces. When preparing the lookup table, the land use types were made compatible with the input needs of the model. The prepared land uses map was given as input to the model. The data used for model setup and analysis are also summarized in Table 3.4.

Table 3.4: Data used for model setup, calibration, validation and scenario analysis

Data	Resolution	Source
Nine Stations Observed stream flow	1995-2010	National Meteorology Agency of Ethiopia
Climate	2006-2060	ICHEC-EC-EARTH
Gauging Station	1995-2010	Ministry of Water, Irrigation & Energy of Ethiopia
Digital Elevation Model (DEM) (SRTM)	30 m	Shuttle Radar Topography Mission
Land use 2000	30m	GlobeLand30
Soil	30 arc-second	Harmonized World Soil Database v 1.2

The look up table containing many SWAT land cover/use codes was used to connect the SWAT land use data base the land use layer in .txt format as shown in Table 3.5.

Table 3.5: LULC classification of Gidabo catchment

OBJECTID	gridcode	%	Shape_Area	Code	Landuse
1	10	65.00	1713.27	10	Agricultural
2	20	32.37	853.26	20	Forest
3	30	1.87	49.23	30	Grassland
4	40	0.06	1.62	40	Shrubland
6	60	0.00	0.01	60	Water bodies
7	80	0.62	16.31	80	Artificial Surfaces/Urban
8	90	0.08	2.07	90	Bare Land

3.6. Model Setup

3.6.1. Watershed Delineation

After model input preparation model setup was the next step. The data base containing user soils and weather generator was copied to the new folder which contains all the necessary input data. The watershed delineation was performed using 30 m resolution DEM using Arc SWAT 12 watershed delineator. First the SWAT project setup was created using the folder contain all input data and SWAT12.mdb database.

The watershed delineation process consists of six major steps, DEM setup, stream definition, and outlet and inlet definition, watershed outlet selection and adding reservoir and calculation of sub basin parameter. The stream definition and the size of sub basin were determined by using threshold area 4000 hectares. User selected threshold stream definition plays important role in determining the detail of the stream network and the size and number of watershed. The smaller the number of hectares the more detailed the drainage network delineated.

The Gidabo River Catchment was delineated in to 51 sub basin with an area of 2635km^2 by selecting the outlet in the Measso station. During the watershed delineation process the elevation of the watershed ranges from 1200 to 3200 a.m.s.l. The description of the delineation process is described in the flowing section.

Outlet Definition Introducing DEM data to the model was the first step. The DEM was projected to Universal Transverse Mercator under zone 37N in Spheroid of WGS_1984. After DEM data was processed stream definition was the next step, in stream definition initial stream network and sub-basin outlet were defined.

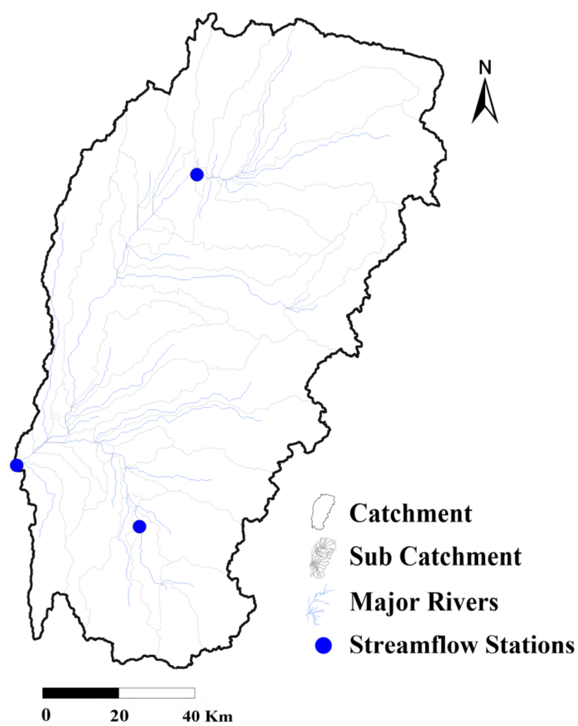

Figure 3.7: Location of stream flow gauges sub-basins on Gidabo Basin

Watershed delineation is more refined by defining the outlet point of discharge for the sub-basin and for the whole watershed. The location of the stream flow gauges and Gidabo River axis were connected to the interface using the data base table see Fig.3.7. The watershed outlet was defined manually in Measso station.

3.6.2. Defining Land Use/Soil Data and Slope

Land use, soil map and slope were overlaid for each sub-basin, which forms the basis for the formation of Hydrological Response Units (Neitsch et al., 2011).

3.6.3. HRU Definition

After the overlay of the land use, soil and slope maps was completed the next step was HRU definition. Dividing the watershed in to unique land use, soil and slope combinations help the SWAT model to reflect difference in hydrological conditions for the different land use, soil and slope. There are two options in the model to define HRU. The first one is a single HRU to each sub-watershed and the second one is multiple HRUS to each sub watershed based on threshold values. Threshold value is used to remove minor land use/covers in sub basins, minor soil with in a land use/cover area and minor slope classes in a soil classes with in a soil on specific land use/cover area (Asmamaw, 2013). The overall input, process and parameterization of data is presented in Figure 3.8.

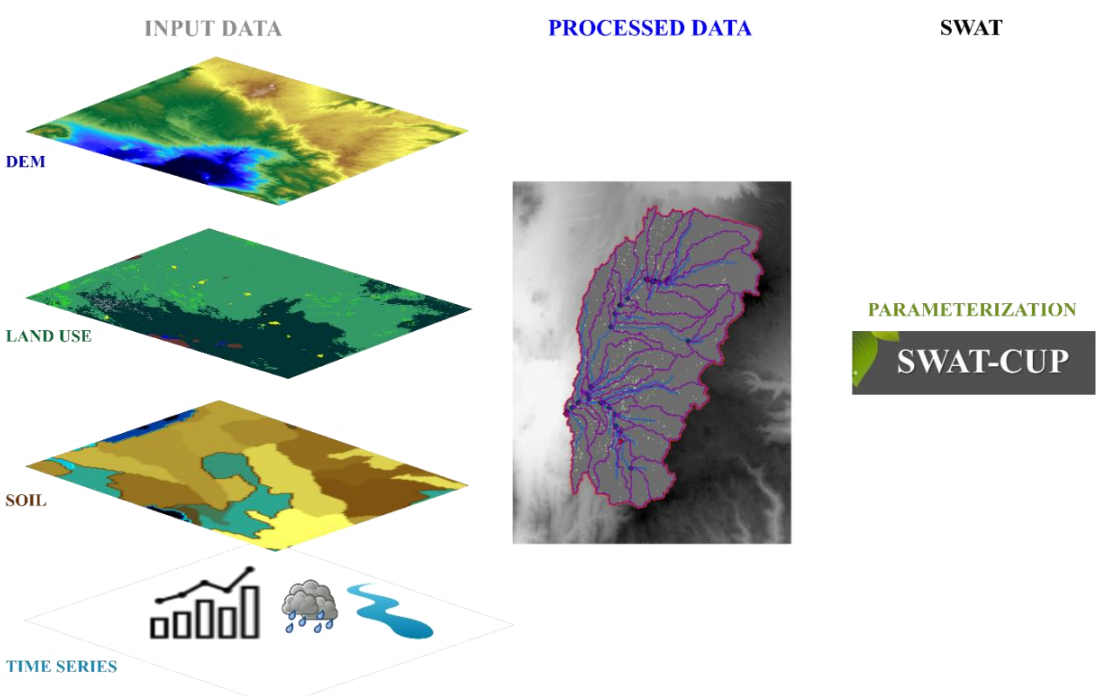

Figure 3.8: The overall input, process and parameterization of data

For this study multiple options and 5% land use threshold, 10% soil threshold and 10% slope threshold was used for HRU definition. This means minor land use less than 5% in sub-watershed was removed, minor soil less than 10% in a land use was removed and minor slope classes less than 10% in a soil classes with in specific land use/cover was removed. The Gidabo River Catchment was divided in to 563 HRUs and 51 sub-basins, each HRU contain unique land use, soil and slope combinations.

After HRUs definition, daily values of precipitation, maximum and minimum temperature, solar radiation, relative humidity and wind speed were provided to define weather data base. Rainfall data for the 9 gauging locations was provided, which contains locations of the rain gauge. The gauge location .txt file and the .txt file which contained the daily values are in the same folder for each gauge locations. Temperature, wind relative humidity and solar radiation also provided to the model using the gauge location .txt file, these files and the daily data of the climatic variables also in the same folder. The missing values were generated from monthly average climatic data by WGN maker 4.1 weather generator model.

3.7. Sensitivity Analysis, Calibration, Validation and Uncertainty Analysis

SWAT-CUP enables sensitivity analysis, calibration, validation and uncertainty of SWAT models. Automated model calibration requires that the uncertain model parameters are systematically changed, the model is run and the required outputs (corresponding to measured data) are extracted from the model output files (Abbaspour, 2015).

Synchronizing SWAT execution file version between Arc SWAT 12 and SWAT-CUP was the first step before the calibration process. SWAT exe file (SWAT_32rel.exe) was copied from the Arc SWAT 12 installation directory and pasted in SWAT-CUP installation directory then the SWAT_32rel.exe file renamed to swat.exe. The oldswat.exe in the SWAT-CUP installation directory renamed to swat_old.exe.

3.7.1. Sensitivity Analysis

Sensitivity can be defined as the process of determining the rate of change in the SWAT model output to changes in parameters (model input). Two kind of sensitivity analysis was performed (Abbaspour, 2015). These are Global and one-at-time sensitivity analysis. In this study, the global sensitivity performed by SUFI-2 was examined. Global sensitivity estimates the average changes in the objective function from changes in each parameter, while all other parameters are changing. Global sensitivity requires larger simulation (Perry, 2015).

Table 3.6: List of parameters and their initial ranges used for model calibration of stream flow

Parameter Name	Description	Range	
		Min	Max
v_ALPHA BF.gw	Base flow alpha factor(days)	0	1
v_CN2().mgt	SCS runoff curve number for moisture condition II	35	98
v GW DELAY.g	Ground water delay time (days)	30	450
v GW QMN.gw	Threshold depth of water in shallow aquifer for return flow to occur (mm)	0	5000
v GW REVAP.gw	Ground water revap. Coefficient	0.02	0.2
v RCHRG DP.gw	Deep aquifer percolation fraction	0	1
v REVAPMN. gw	Threshold depth of water in the shallow aquifer for "revap" to occur (mm)	0	500
v SLSUBBSN.hru	Average slope length (m)	10	150
v ESCO.hru	Soil evaporation compensation factor	0	1
v CANMX.hru	Maximum canopy storage	0	10
v CH_K2.rte	Effective hydraulic conductivity in the main channel (mm h-1)	0	150
r SOL_AWC().sol	Soil available water storage capacity (mm H2O/mm soil)	-0.25	0.25
r__SOL_K().sol	Soil conductivity (mm h-1)	-0.25	0.25
r__SOL_Z().sol	Maximum rooting depth of soil profile (m)	-0.25	0.25
v__HRU_SLP.hru	Average slope steepness (mm-1)	0	0.6

Relative (r __) means the existing parameter value is multiplied by (1+ a given value).
Replace (v __) means the existing parameter value is to be replaced by the given value.

3.7.2. Calibration, Validation and Uncertainty Analysis

Sensitivity, calibration, validation and uncertainty were performed for stream flow and sediment yield using river discharge and sediment load. SUFI-2 was used for calibration and uncertainty analysis. Calibration is model testing with known measured output, and adjusting parameters for the most sensitive once which will result in a more accurate representation of the system being modeled (Perry, 2015).

In SUFI-2, all sources of uncertainties are mapped to a set of parameter ranges. They are calibrated with the aim of bracketing most of the observed data with as narrow as possible in uncertainty band (Abbaspour et al., 2014). Initially, a set of parameter ranges are assigned to calibrating parameters based on literature (Abbaspour et al., 2014; Abraham et al., 2015) and sensitivity analyses.

The uncertainty is quantified at the 2.5% and 97.5% levels of the cumulative frequency distribution of all simulated output values, and it is referred to as the 95% prediction uncertainty (95PPU). The lower, middle, and upper boundaries of the 95PPU (L95PPU, M95PPU, and U95PPU) reflect the 2.5, 50, and 97.5 percentiles of the distribution, respectively (Abbaspour, 2015).

The model performance in terms of calibration and uncertainty level is evaluated using the p-factor and the r-factor. The p-factor is the percentage of measured data bracketed by the 95PPU band. It ranges from 0 to 1 where 1 means all of the measured data are within the uncertainty band (i.e., model prediction).The r-factor is the average width of the band divided by the standard deviation of the measured variable. It ranges from 0 to ∞ (Abbaspour et al., 2014). Based on source of data the calibration period was from 1995 to 2007. Model was run on the monthly basis using 3 years NYSKIP (numbers of years skip for model warm up).

The program was simulated 500 times for 5 iterations for stream flow parameters. When acceptable values of r-factor and p-factor are reached, then the parameter uncertainties are the desired parameter ranges. Further goodness of fit can be quantified by the R^2 and Nash-Sutcliff (NS) coefficient between the observations and the final “best” simulation (Abbaspour, 2015). The final step after calibration is the validation process.

Validation process demonstrates that the model is capable of making sufficiently accurate simulations (Perry, 2015). The validation period was from 2008 to 2010 and the calibrated parameter range and number of simulation was used in the validation process Table 3.5 shows parameters used for calibration of stream flow and their initial ranges and the way they are adjusted in the SWAT-CUP. The type of change applied for the parameter was based on the SWAT-CUP manual (Abbaspour, 2015).

3.7.3. Model Efficiency Evaluation

For model performance evaluation both graphical techniques and quantitative statistical analysis should be used to compare the measured data to the simulated data (Moriasi et al., 2007). In this study graphical techniques, coefficient of determination (R2), Nash-Sutcliffe Efficiency (NSE) and percent BIAS were used.

The Coefficient of Determination R^2: value is an indicator of strength of relationship between the observed and simulated values. It indicates how well the dispersion of the measured data is predicted by the model. Its value ranges between 0 and 1, with the zero being no correlation at all and value of one indicates perfect match. The more it approaches to 1 the more correlation between observed and simulated the value of R^2 greater than 0.5 are considered to be acceptable (Perry, 2015). R^2 is computed as shown in the equation 3.5

Error! Reference source not found.Error! Reference source not found.

(3.12)

Where

Q_{sim} = Q stimulated

Q_{obs} = Q Observed

The Nash-Sutcliffe Simulation Efficiency (NSE): NSE is an indication of how well the plot of observed versus simulated data fits the 1:1 line. If the measured value is the same as all prediction, NSE is one. If NSE is between 0 and 1, it indicates deviations between measured and predicted values. If ENS is negative, predictions are very poor, and average value of output is better estimate than the model prediction. NSE is computed using equation 3.13. The ranges of NSE is between -∞ and 1. The model simulation can be judged as satisfactory if NSE>0.5 (Moriasi et al., 2007).

Error! Reference source not found. *(3.13)*

Where Yi_{obs} is the i^{th} observation for the constituent being evaluated, Yi_{sim} is the i^{th} simulated value for the constituent being evaluated, Ymean is the mean of observed data for the constituent being evaluated, and n is the total number of observations (Moriasi et al., 2007).

Percent Bias (PBIAS): PBIAS measure the average tendency of the simulated data to be larger or smaller than their observed counterparts. The optimal value of PBIAS is zero, with low magnitude values indicating accurate model simulation. Positive values indicate model underestimation bias, and negative values indicate model over estimation. If PBIAS value of ±10 %< PBIAS<±15% is achieved in flow calibration or validation then the model performance is good (Moriasi et al., 2007).

Error! Reference source not found. *(3.14)*

Where: n is the number of observations during simulation period, Q_{obs} is the observed flow, Q_{sim} is simulated flow with respect to time

Table 3.7: Performance ratings for different statistical indices (Moriasi et al., 2007).

Performance Rating	R^2	E_{NS}	PBIAS (%)
Very good	$0.75 < R^2 \leq 1$	$0.75 < NSE \leq 1.00$	$PBIAS \leq \pm 10.0$
Adequate/good	$0.60 < R^2 \leq 0.75$	$0.65 < NSE \leq 0.75$	$\pm 10 \leq PBIAS < \pm 15$
Satisfactory	$0.50 < R^2 \leq 0.60$	$0.50 \leq NSE \leq 0.65$	$\pm 15 \leq PBIAS < \pm 25$
Unsatisfactory	$R^2 < 0.50$	$NSE < 0.50$	$PBIAS \geq \pm 25$

4. RESULT AND DISCUSSIONS

4.1. Sensitivity Analysis

The results of a sensitivity analysis can be used to eliminate non-sensitive parameters from the calibration process. First the initial range of parameters was assigned based on literature and SWAT absolute values see table 3.5. The t-statistic gives a measure of the sensitivity of the parameter. The p-values show the significance of the sensitivity. The larger absolute value of t-stat shows more sensitive and the smaller p-values indicates higher significance of the sensitivity.

The most sensitive parameter is the SOL_AWC for the selected 3 sub-basins and the sensitivity is highly significant (p-value=0). Next to SOL_AWC CN2, HRU_SLP, RCHRG_DP, GWQMN and ALPHA_BF are the next sensitive parameters for the land use maps. The majority of the other parameters where also significantly sensitive (close to or equal to zero) all the parameters were used during calibration in SUFI-2.The only problem using greater number of parameters in calibration would be time that the SWAT-CUP takes to run the iteration (one iteration means in this case 500 simulations). For this study all parameters were chosen and the run time could be short if less parameter were used but not much. Based on the global sensitivity results and one-at-time sensitivity analysis the final calibrated parameter range was obtained see Table 4.1 and Figure 4.1.

Table 4.1 Results of sensitivity analysis for flow parameter for SUFI-2.

Parameter_Name	Fitted_Value	Min_value	Max_value
1:V__CN2.mgt	69.79	64.75	81.46
2:V__GWQMN.gw	7671.22	4630.57	7739.62
3:V__RCHRG_DP.gw	0.24	-0.10	0.34
4:V__ALPHA_BF.gw	0.39	0.18	0.43
5:V__CANMX.hru	-1.46	-6.13	0.34
6:V__ESCO.hru	-0.16	-0.88	-0.16
7:V__CH_K2.rte	207.81	183.01	268.53
8:R__SOL_AWC(..).sol	0.40	0.38	0.64
9:R__SOL_Z(..).sol	-0.02	-0.06	0.04
10:V__SLSUBBSN.hru	-18.50	-57.15	7.49
11:V__HRU_SLP.hru	0.48	0.37	0.56

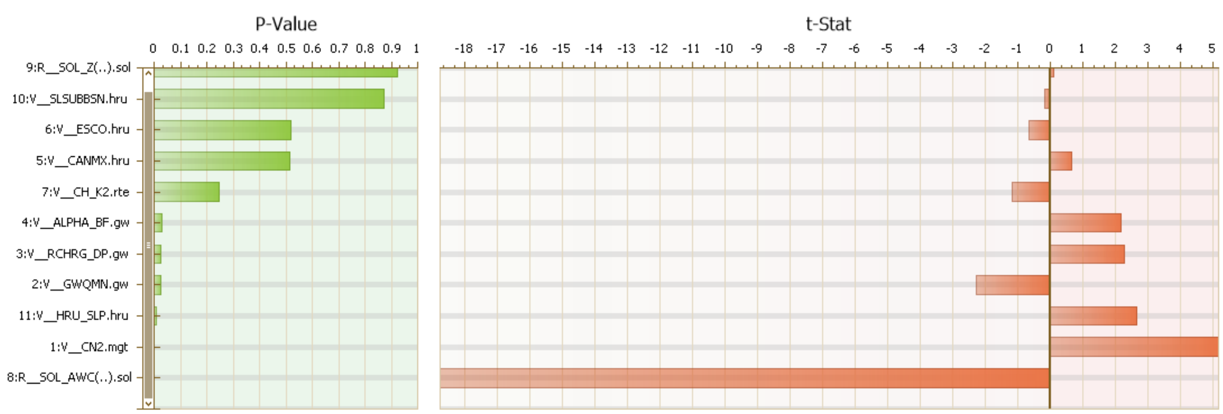

Figure 4.1: Result of sensitivity analysis for flow parameters on SWAT CUP (SUFI-2)

4.2. SWAT Model Calibration and Validation

To improve the efficiency of the model during calibration the top eleven ranking parameters were considered to account for the over and under prediction responses of the model as suggested by Neitsch et al. (2011). Model calibrations were computed using 1998-2007 climate data against measured discharge data. Model validation consist the comparison of the model outputs with an independent data set without making further adjustments of the parameters obtained during the calibration process. Using the same parameter values the calibrated model setup were validated and found to prove the applicability and result acceptable performance. Model validation was performed from 2008 to 2010 against the measured due date value.

The result of calibration in successive iteration with 500 simulations in Aposto station which is located in sub-basin 7 showed acceptable p-factor and r-factor. With p-factor of 0.56 and r-factor of 0.51 which shows the 95ppu band see Fig 4.2. For model performance evaluation that measure the agreement between measured stream flow and simulated flow NSE, PBIAS and R^2 were used as criteria. The objective function in SWAT-CUP was specified as NSE>0.5 and the result of the calibration was 0.69 based on (Moriasi et al., 2007) performance ratings for monthly time step NSE value of $0.65 < NSE < 0.75$ indicate good model performance in Aposto station. Other statistical measures comparing the simulated data to the observed data in SUFI-2 are presented in Table 4.2. These includes correlation R^2 which is 0.73 and this shows good correlation and PBIAS value is 12.6 which indicate very good performance (Moriasi et al., 2007).

For validation period (2008-2010) p-factor 0.47 with r-factor of 0.65 which is acceptable (Abbaspour et.al, 2015). The goodness of fit between observed and simulated flow for validation period showed very good result with NSE value of 0.60. The Correlation coefficient R^2 between observed and simulated flow showed good correlation with value of 0.64 and Pbias of 9.5 which is a very good correlation with the observed value.

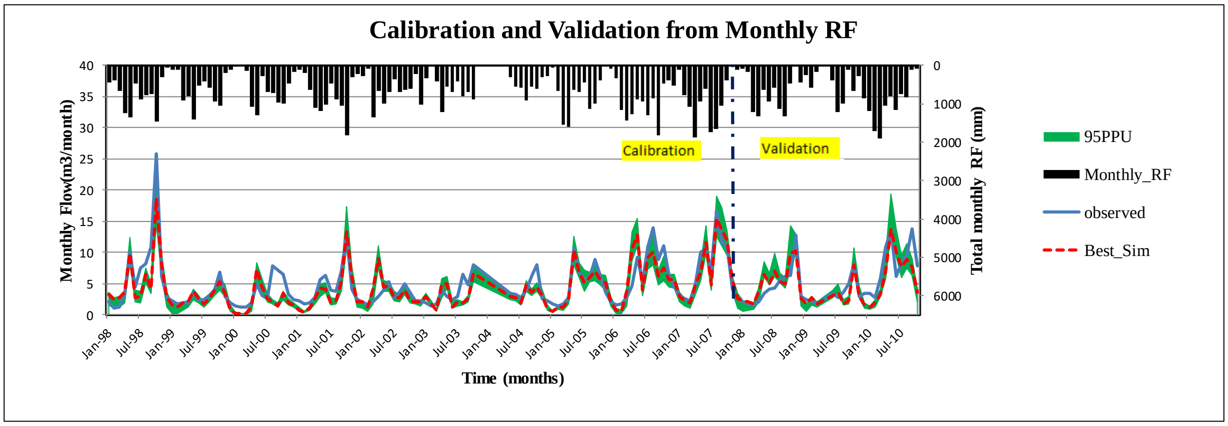

Figure 4.2: Illustration of full SWAT-CUP output for calibration period of 1998-2007 and for Validation period of 2008-2010 the observed, best simulation and 95% prediction uncertainty (95PPU) and monthly rainfall for Aposto outlets.

Flow calibration in Measso station (Gidabo River Catchment outlet) showed acceptable result both for p-factor and r-factor. The p-factor of 0.84 which means 84% of the observed data is captured by the 95PPU with r-factor of 0.83 which is acceptable see Fig 4.3. The correlation between observed and simulated flows showed a good agreement with the value of R^2 0.84, and NSE value of 0.84 which fell in very good model performance range (Abbaspour, 2015).

For validation period 0.73 percent of the observed data is captured by 95PPU band with r-factor of 0.65. The model performance result in Measso station showed satisfactory result with value of NSE 0.63 which is acceptable value. The coefficient of correlation also showed good agreement between the observed and the simulated stream flow with the value of 0.63.

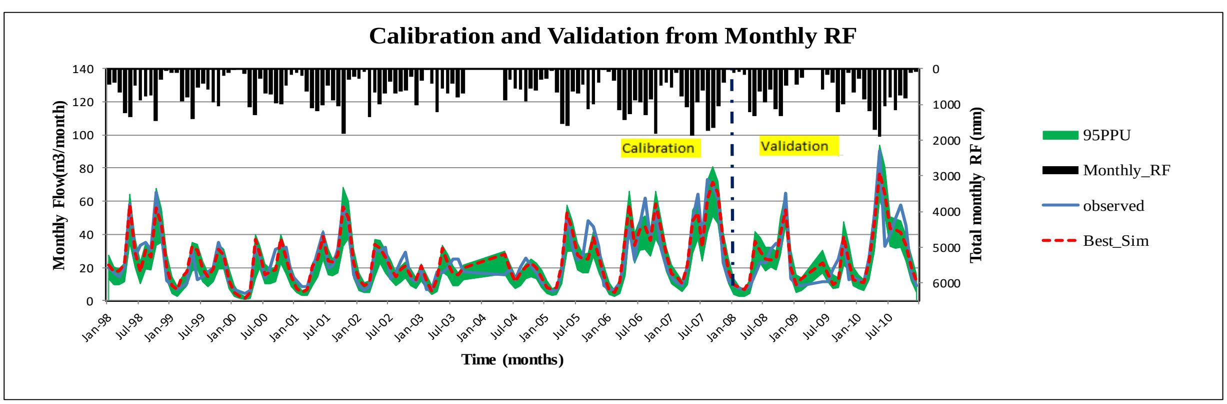

Figure 4.3: Illustration of full SWAT-CUP output for calibration period of 1998-2007 and for Validation period of 2008-2010 the observed, best simulation and 95% prediction uncertainty (95PPU) and monthly rainfall for Measso/Gidabo River Catchment outlet.

Flow calibration in Bedessa station showed acceptable result in the calibration period. The p-factor of 0.59 which is 59% of the observed data is captured by the model output or 95ppu with r-factor of 0.85 which is smaller band. Both p-factor and r-factor are acceptable (Perry, 2015; Abbaspour et.al, 2015). Other statistical criterion measure the agreement between the measured signal and the simulated signal also showed satisfactory results. These are correlation R^2 which is 0.65, NSE 0.65 and PBIAS -3.7 see Fig 4.4 and Table 4.2.

Using the calibrated parameter and the same number of simulation validation of flow variable was conducted .the results of validation in Bedessa gauged station showed that 41% of the observed data was captured by the 95ppu with smaller band which means r- factor 0.86 see Table 4.3. The R^2 value showed satisfactory model performance results with value of 0.50. Based on the result, the model is efficient enough to represent and evaluate the impact of climate change on stream flow variability.

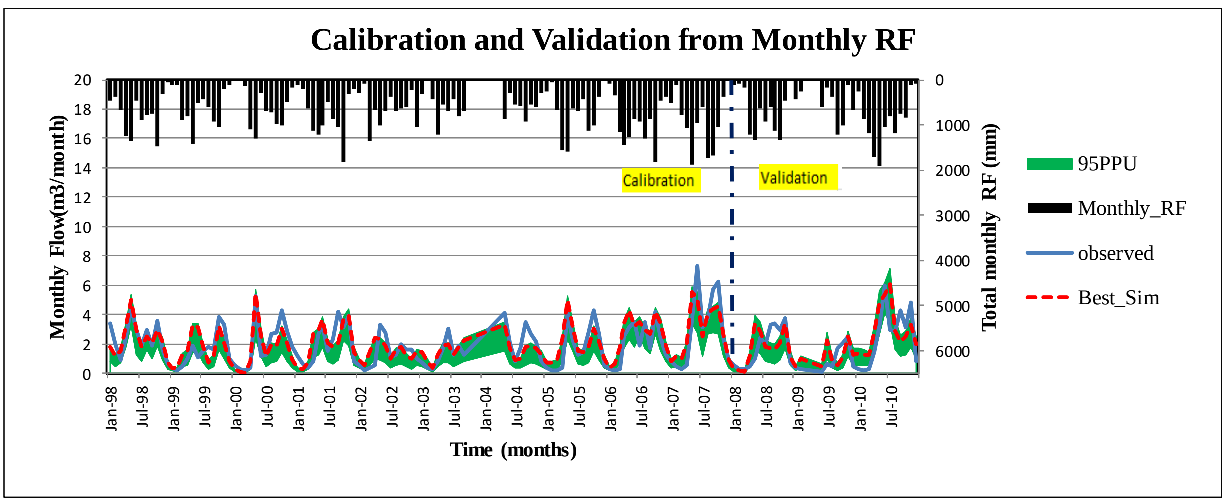

Figure 4.4: Illustration of full SWAT-CUP output for calibration period of 1998-2007 and for Validation period of 2008-2010 the observed, best simulation and 95% prediction uncertainty (95PPU) and monthly rainfall for Bedessa outlet.

Table 4.2: output file of SWAT-CUP Summary statistics for calibration period of 1998-2010

Goal_type= Nash_Sutcliff   No_sims= 500   Best_sim_no= 176   Best_goal = 7.276173e-001

Variable	p-factor	r-factor	R2	NS	bR2	MSE	SSQR	PBIAS	KGE	RSR	MNS	VOL_FR
FLOW_OUT_7	0.56	0.51	0.73	0.69	0.5682	4.3e+000	9.2e-001	12.6	0.79	0.55	0.49	1.14
FLOW_OUT_39	0.83	0.84	0.84	0.84	0.7334	4.0e+001	3.0e+000	-1.5	0.90	0.40	0.63	0.99
FLOW_OUT_48	0.58	0.88	0.65	0.65	0.4488	7.6e-001	9.7e-002	-3.7	0.75	0.59	0.43	0.96

Table 4.3: output file of SWAT-CUP Summary statistics for validation period of 2008-2010

Goal_type= Nash_Sutcliff   No_sims= 500   Best_sim_no= 214   Best_goal = 5.599261e-001

Variable	p-factor	r-factor	R2	NS	bR2	MSE	SSQR	PBIAS	KGE	RSR	MNS	VOL_FR
FLOW_OUT_7	0.47	0.65	0.64	0.60	0.4766	4.7e+000	7.6e-001	9.5	0.77	0.63	0.43	1.11
FLOW_OUT_39	0.73	0.65	0.63	0.63	0.3853	1.9e+002	4.6e+001	2.6	0.69	0.61	0.52	1.03
FLOW_OUT_48	0.41	0.86	0.50	0.44	0.3250	1.4e+000	1.6e-001	-10.8	0.68	0.75	0.33	0.90

4.3. Projected Future Climate Variables

4.3.1. Annual and Monthly Mean Maximum Temperature Changes

The mean annual and monthly maximum temperature increases for all Ensemble mean of CCLM4, RCA4, RACMO22T and REMO2009 regional climate models for both RCP scenarios in the 2020s and 2050s compared to the baseline (1995–2005). For the Ensemble mean of the highest increases of mean monthly temperature by 0.76 °C for RCP4.5 and 0.85 °C for RCP8.5 in the 2020s and for the mid-term period 1.78 °C for RCP4.5 and 2.3 °C for RCP8.5 in the 2050s (see Fig 4.5).

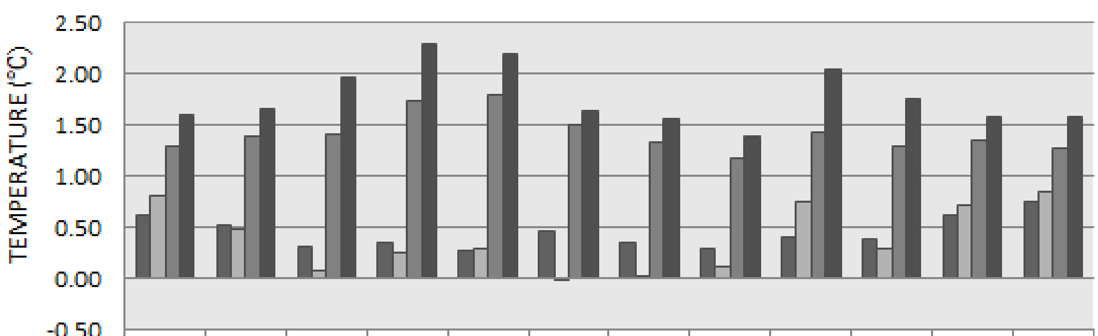

	Jan	Feb	Mar	Apr	May	Jun	Jul	Aug	Sep	Oct	Nov	Dec
RCP4.5_20'S	0.62	0.51	0.30	0.35	0.28	0.46	0.35	0.29	0.40	0.39	0.62	0.76
RCP8.5_20'S	0.81	0.48	0.08	0.26	0.29	-0.02	0.00	0.11	0.76	0.30	0.72	0.85
RCP4.5_50'S	1.29	1.38	1.42	1.73	1.79	1.51	1.33	1.19	1.42	1.30	1.35	1.27
RCP8.5_50'S	1.59	1.66	1.97	2.30	2.20	1.63	1.57	1.39	2.03	1.75	1.58	1.58

Figure 4.5: Mean monthly maximum temperature changes (in the 2020s and 2050s) for RCP4.5 and RCP8.5 scenarios

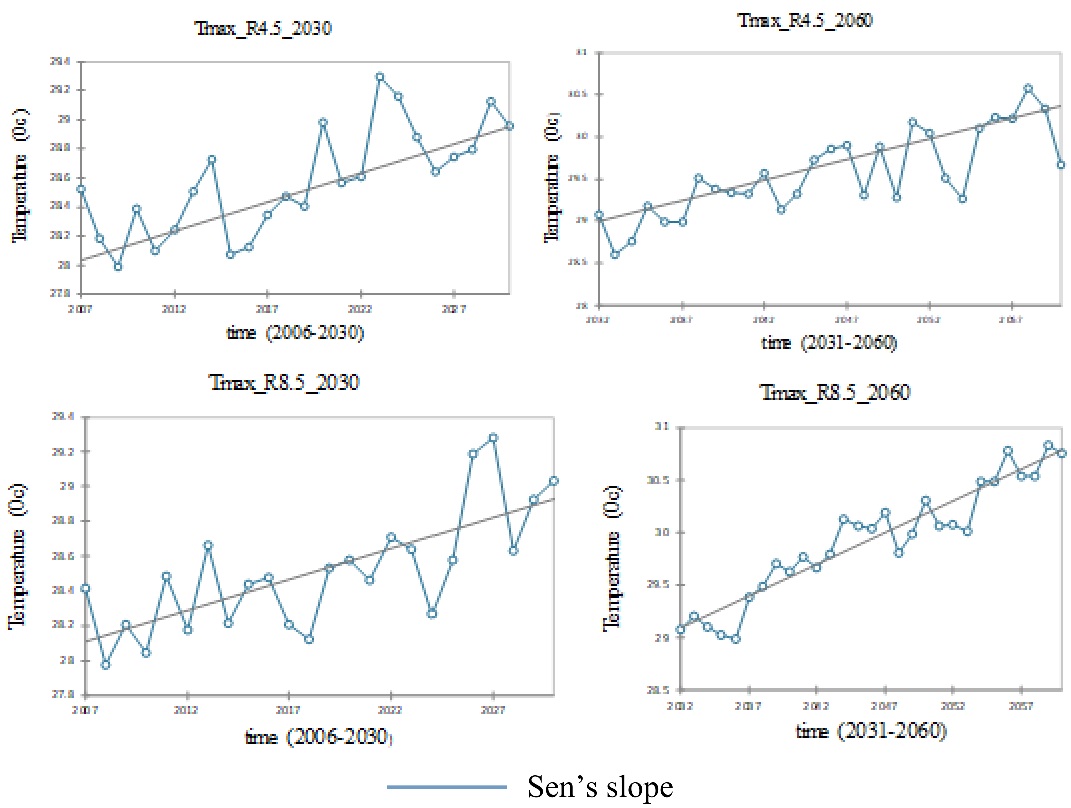

Figure 4.6: Trends of projected mean annual maximum temperature for RCP4.5 and RCP8.5 over Gidabo catchment

The variability of temperature is higher for all ENSEMBLEs in the RCP8.5 than RCP4.5 scenarios and the future trend in the RCP8.5 and RCP4.5 scenarios have indicated a statistically significant (at 5% significant level) increasing trend for mean annual temperature and until the end of the century. Furthermore, the result were presented in Fig 4.6 and Table 4.4. Maximum amount of temperature change from RCP 8.5 is because RCP 8.5 produces more greenhouse gas as compared to RCP 4.5, which is medium in greenhouse gas production (Riahi K. et al., 2011).

Table 4.4: Mann Kendall test statistics result for precipitation, minimum and maximum temperature

Minimum Temperature				
Scenarios_yr	Rcp4.5_30	Rcp4.5_60	Rcp8.5_30	Rcp8.5_60
Kendall's tau	0.43	0.56	0.28	0.77
S	118	228	76	312
Var(S)	1625.3	2842	1625.3	2842
Z	2.95	4.30	1.91	5.87
Maximum Temperature				
Scenarios_yr	R4.5_30	R4.5_60	R8.5_30	R8.5_60
Kendall's tau	0.56	0.60	0.56	0.80
S	154	242	154	326
Var(S)	1625.3	2842	1625.3	2842
Z	3.84	4.56	3.84	6.13
Precipitation				
Scenarios_yr	R4.5_30	R4.5_60	R8.5_30	R8.5_60
Kendall's tau	-0.17	-0.13	0.01	-0.12
S	-46	-54	2	-48
Var(S)	1625.3	2842	1625.3	2842
Z	-1.17	-1.03	0.07	-0.92

4.3.2. Annual and Monthly Mean Minimum Temperature Changes

The projected minimum temperature showed that an increment of annual average mean monthly temperature for the Ensemble mean by 0.82 °C for RCP4.5 and 1.06 °C for RCP8.5 in the 2020s and for the mid-term period 1.58 °C for RCP4.5 and 2.16 °C for RCP8.5 in the 2050s. The future trend in the RCP8.5 and RCP4.5 scenarios have indicated a statistically significant (at 5% significant level) increasing trend until the end of the century ,except for, RCP8.5 in 2050s an increasing trend but not statistically significant (at 5% significant level) was observed see Mann Kendall test statistical result presented in Fig 4.8 and Table 4.4.

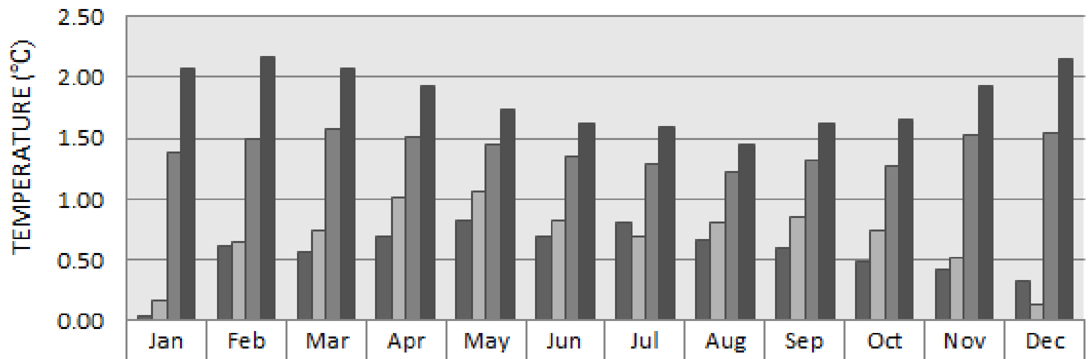

	Jan	Feb	Mar	Apr	May	Jun	Jul	Aug	Sep	Oct	Nov	Dec
RCP4.5_20'S	0.04	0.61	0.56	0.70	0.82	0.69	0.81	0.66	0.60	0.48	0.43	0.33
RCP8.5_20'S	0.16	0.65	0.74	1.01	1.06	0.82	0.70	0.80	0.86	0.74	0.51	0.13
RCP4.5_50'S	1.39	1.49	1.58	1.51	1.44	1.34	1.28	1.22	1.32	1.27	1.53	1.55
RCP8.5_50'S	2.08	2.16	2.07	1.93	1.74	1.62	1.60	1.45	1.62	1.66	1.93	2.15

Figure 4.7: Mean monthly minimum temperature changes (in the 2020s and 2050s) for RCP4.5 and RCP8.5 scenarios

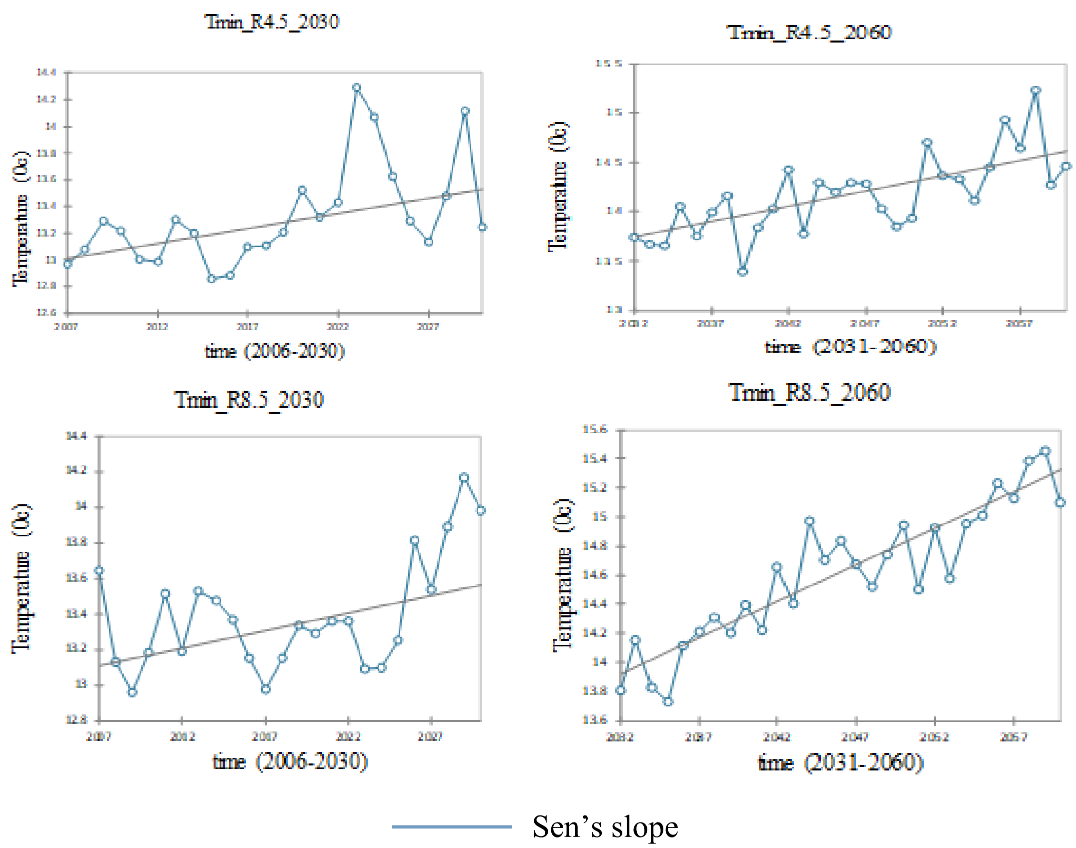

Figure 4.8: Trends of projected mean annual minimum temperature for RCP4.5 and RCP8.5 over Gidabo catchment

The temperature change projection for Gidabo catchment does not in line with the range produced by other researcher by M. Belihu et al., (2017) which concluded that the minimum and maximum temperature trend was magnitude of change reaches 0.08 °C/yr and the mean values proved that the catchment was warming about 0.03 °C/yr to 0.07 °C/yr. The result of this study presented in Fig 4.7. As a result, the same conclusion has reached upon like the case of maximum temperature, where minimum temperature change also exceeds for RCP 8.5 than RCP 4.5 due to the fact that, RCP 8.5 represents high emission scenario which produces more greenhouse gas as compared to RCP 4.5 (Riahi K. et al., 2011).

4.3.3. Annual and Monthly Mean Precipitation Changes

The climate models simulations exhibit a mixed monthly precipitation change signal between reference period (1995-2005) and near-term period (2006-2030) and mid-term period (2031-2060) see the result in Fig 4.9. For both scenario RCP4.5 and RCP8.5 exhibit mixed signals in the direction of monthly precipitation change. The overall result revealed that, percentage change in monthly average precipitation might range between 5% to 18% for all months except for April, August, September, and November which was reduced by -3% to 16% during 2020's and 2050's.

As described in the IPCC Third Assessment Report (McCarthy et al., 2001), the projected future changes in mean seasonal rainfall in Africa are less well defined. The diversity of African climates, high rainfall variability, and a very sparse observational network make the predictions of future climate change difficult at the sub regional and local scales. Under intermediate warming scenarios, rainfall is predicted to increase in December-February and decrease in June-August in parts of East Africa. With a more rapid global warming scenario, large areas of Africa would experience changes in December-February or June-August rainfall that exceed natural variability. With reference to this study rainfall will also experience a increment in June-July for most part of the future time horizons. However, the rainfall variation is not significant because of $Z\alpha < 1.96$ in Mk trend test result of the annual rainfall in the study area (Fig 4.10 and table 4.4).

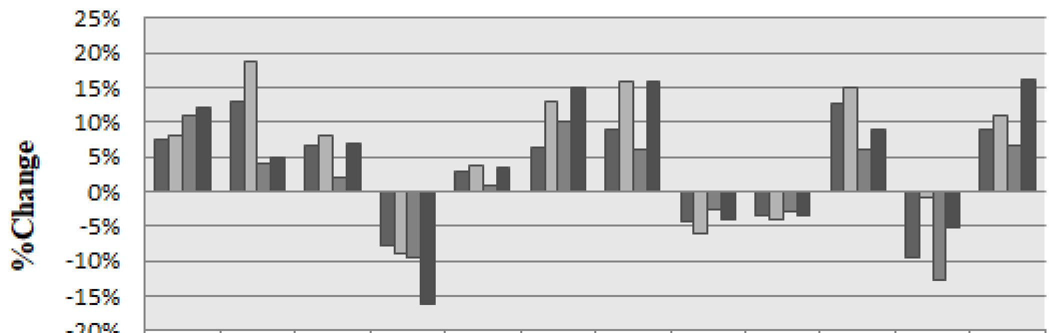

	Jan	Feb	Mar	Apr	May	Jun	Jul	Aug	Sep	Oct	Nov	Dec
%change_R4.5_20'S	7%	13%	7%	-8%	3%	6%	9%	-4%	-4%	13%	-10%	9%
%change_R8.5_20'S	8%	19%	8%	-9%	4%	13%	16%	-6%	-4%	15%	-1%	11%
%change_R4.5_50'S	11%	4%	2%	-10%	1%	10%	6%	-3%	-3%	6%	-13%	7%
%change_R8.5_50'S	12%	5%	7%	-16%	3%	15%	16%	-4%	-3%	9%	-5%	16%

Figure 4.9: Mean monthly precipitation percentage changes (in the 2020s and 2050s) for RCP4.5 and RCP8.5 scenarios

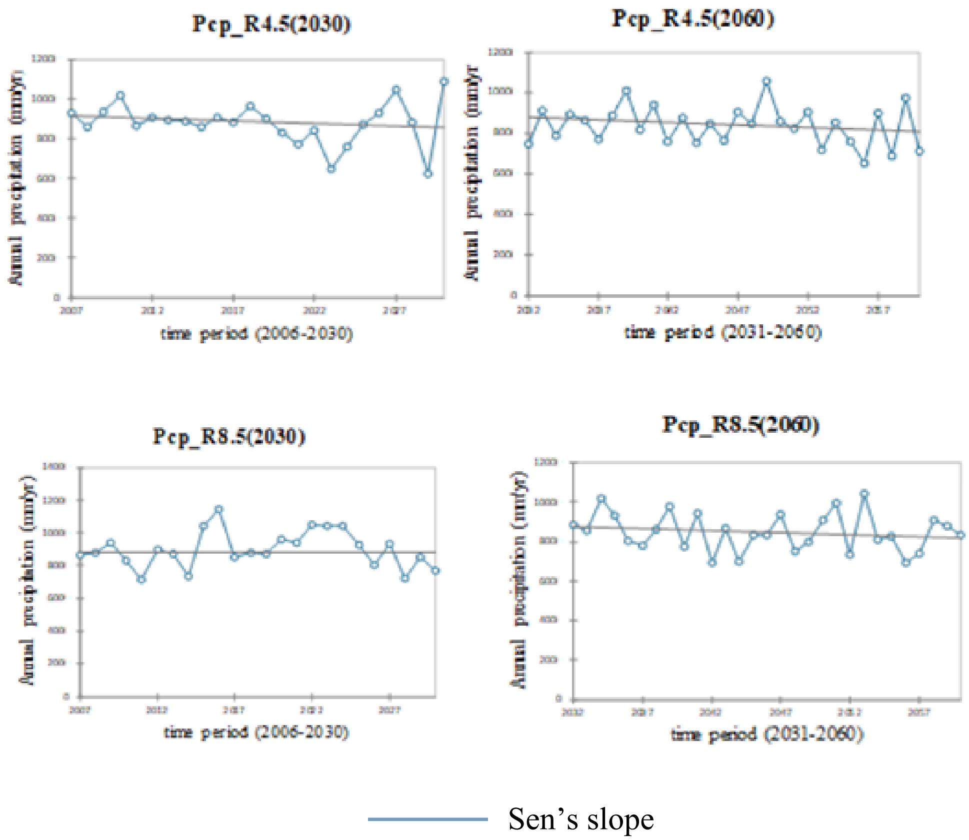

Figure 4.10: Trends of projected annual precipitation for RCP4.5 and RCP8.5 over Gidabo catchment

4.4. Mean Monthly and Annual Change in Streamflow (Net Water Availability)

Water availability shows a mixed change for the near-term and midterm period within both of the representative concentration pathways. Almost all models projected shows increment 5% to 28% water availability in June, July and December under RCP4.5 and RCP8.5 for all time slices, whereas decrement on the rest of the months and time slices (see Fig 4.11 and 4.12). Except for April and May which is a decreases in 2050's and increases 2020's for both scenarios RCP4.5 and Rcp8.5.

The net annual water availability variation is insignificant but decreasing trend according to Mann Kendall test result presented in Fig 4.13 for both scenarios of RCP4.5 and RCP8.5 scenario. The double peaking in net water availability ensues in May and Oct. As we can see from the above results that there has been high monthly variation of water availability as compared to the variation in annual scale for all the RCP scenarios and in all the time slices. Mixed results in direction of streamflow are projected under both scenarios and hence it is not possible to be conclusive in this study. Overall, this study shows the importance of using multiple climate models to understand the range of projected changes in water resource availability in a basin.

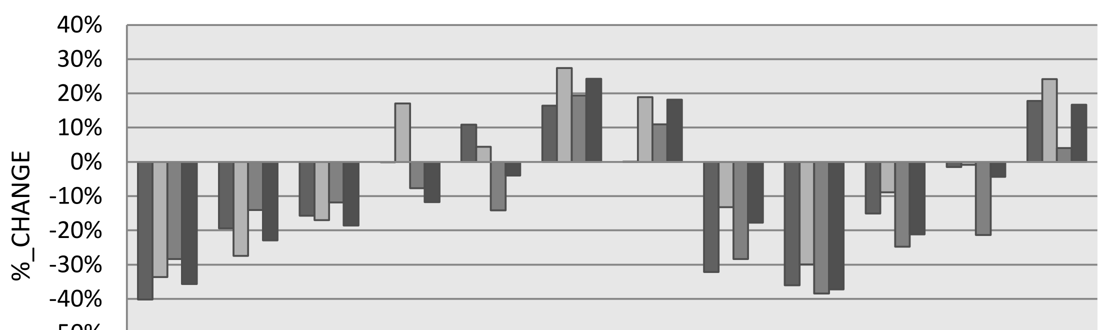

	Jan	Feb	Mar	Apr	May	Jun	Jul	Aug	Sep	Oct	Nov	Dec
RCP4.5_20'S	-40%	-19%	-16%	0%	11%	16%	0%	-32%	-36%	-15%	-1%	18%
RCP8.5_20'S	-34%	-27%	-17%	17%	4%	27%	19%	-13%	-30%	-9%	-1%	24%
RCP4.5_50'S	-28%	-14%	-12%	-8%	-14%	19%	11%	-28%	-38%	-25%	-21%	4%
RCP8.5_50'S	-36%	-23%	-19%	-12%	-4%	24%	18%	-18%	-37%	-21%	-4%	17%

Figure 4.11: Mean monthly stream-flow percentage changes (mean of 4 RCMs) for RCP4.5 and RCP8.5 scenarios

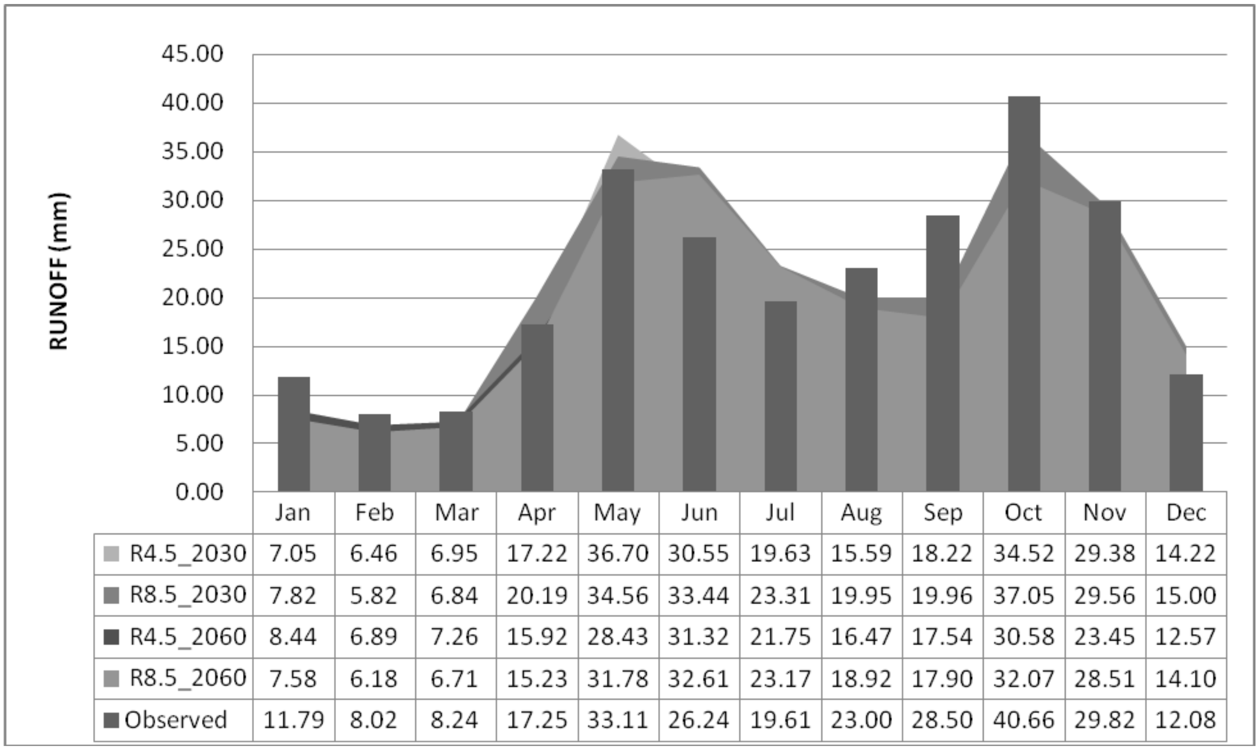

	Jan	Feb	Mar	Apr	May	Jun	Jul	Aug	Sep	Oct	Nov	Dec
R4.5_2030	7.05	6.46	6.95	17.22	36.70	30.55	19.63	15.59	18.22	34.52	29.38	14.22
R8.5_2030	7.82	5.82	6.84	20.19	34.56	33.44	23.31	19.95	19.96	37.05	29.56	15.00
R4.5_2060	8.44	6.89	7.26	15.92	28.43	31.32	21.75	16.47	17.54	30.58	23.45	12.57
R8.5_2060	7.58	6.18	6.71	15.23	31.78	32.61	23.17	18.92	17.90	32.07	28.51	14.10
Observed	11.79	8.02	8.24	17.25	33.11	26.24	19.61	23.00	28.50	40.66	29.82	12.08

Figure 4.12: Baseline and future (mean of 4 RCMs for the two time slices) monthly net water availability for RCP4.5 and RCP8.5 scenarios

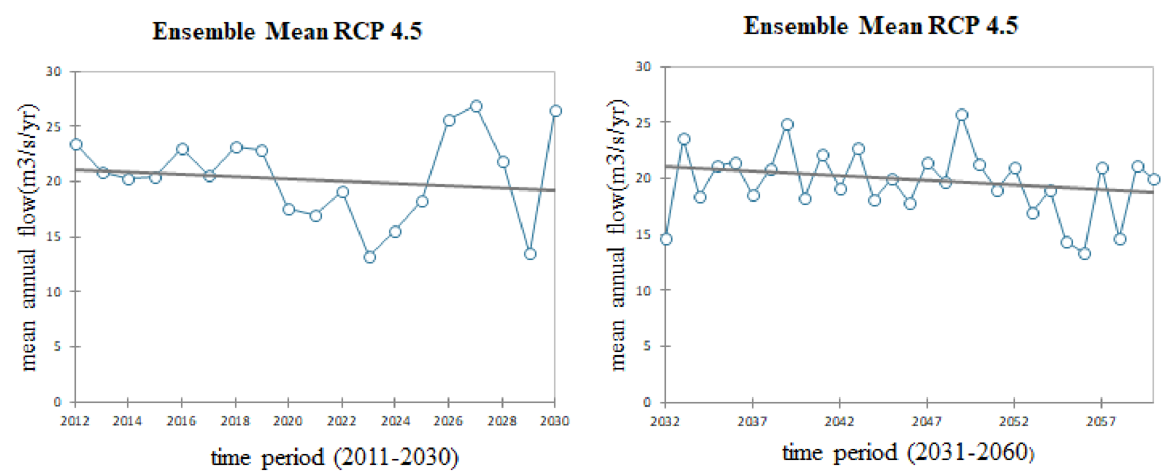

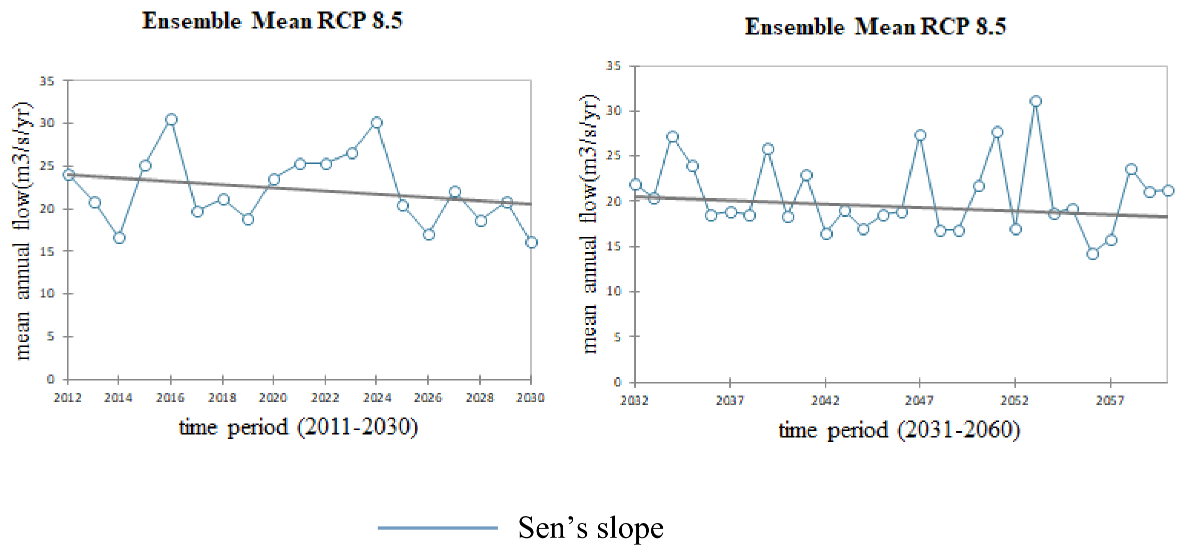

Figure 4.13: Trends of projected mean annual stream-flow for RCP4.5 and RCP8.5 over Gidabo catchment

5. CONCLUSION AND RECOMMENDATION

5.1. Conclusions

Climate change is predicted to have a significant impact on the Gidabo catchment's water availability, according to this research. The outputs of four RCMs, CCLM4, RCA4, RACMO22T, and REMO2009, were used as input to a hydrological simulation model to investigate the impact of climate change on water availability in the Gidabo catchment by the mid-twentieth century, all of which were produced as part of the CORDEX-Africa project.

Shanka A.S., (2017) previously demonstrated that the total average annual runoff in the Gidabo river basin is increasing by up to 3.4 percent, 2.9 percent, and 6.8 percent for HadCM3 A2a and 5.1 percent, 5.6 percent, and 5.8 percent for HadCM3 B2a scenarios, respectively, in the 2020s, 2050s, and 2080s. Unlike earlier studies, the yearly runoff in this research region is decreasing, although not at a substantial level.

Rainfall projections did not show a systematic rise or reduction across all future time horizons, in contrast to maximum and minimum temperature projections, which show a rising trend across all future time horizons for both RCP4.5 and RCP8.5 scenarios.

The study area's observed maximum and minimum temperatures increased by 0.76 °C for RCP4.5 and 0.85 °C for RCP8.5 in the 2020s, and by 1.78 °C for RCP4.5 and 2.3 °C for RCP8.5 in the 2050s for the mid-term period. The reported increase in temperature in the region has a major influence on agricultural operations, notably in terms of soil water demand, as well as increased evapotranspiration, which causes the catchment to lose more water.

The SWAT model accurately replicates streamflow for the research region, according to the results of hydrological model calibration and validation. At the outlet Measso station, the correlation between observed and simulated flows showed a good agreement with R^2 0.84 and NSE 0.84, which fell in the very good model performance range.

The results of synthetic (incremental) scenarios show that the watershed is vulnerable to climate change, particularly temperature changes. Without any changes in rainfall, a 2°C increase in temperature reduces monthly and yearly runoff. There is a growing tendency in both maximum and lowest temperature in comparison to the past, which leads to an increase in evapotranspiration. The analysis of stream flow of Gidabo from 1998-2005 indicates that there is decreasing trend of the annual runoff. However, based on this restricted research, it is impossible to say if the changes are due to major greenhouse-induced climate change in the watershed.

5.2. Recommendation

There are many sources of uncertainty in the hydrological impact scenarios that are in the climate modeling, the method used for transferring the climate signal to meteorological stations, and in the hydrological modeling. The model simulations have not considered land use changes explicitly although, it is likely that changes in land use may interact with climate leading to different projections of future hydrological conditions. As a result, this study should be taken with care and be considered as indication of likely future changes rather than an actual prediction.

The outcome of this study was based on single GCMs and Ensemble of four RCMs. However, it has recommended that to apply different GCMs to make comparison between different models as well as to explore a wide range of climate change scenarios that would result in different hydrological impacts. Hence, this work would be extending in the future by including different GCMs.

The weather stations should be improved both in quality and in quantity in order to improve the performance of the model. For this reason, it is highly recommended to establish good meteorological stations.

Finally, prior to this investigation no similar modeling approach (SWAT with CCLM4, RCA4, RACMO22T, and REMO2009) was available in the country; the tools used here can be transferred to water resources managers in the Gidabo River basin and the methodology can be improved by scientists in the region to reduce future uncertainties using different SWAT parameters and other regional models and emission scenarios.

REFERENCES

Abayneh, A., 2011, Evaluation of climate change impact on extreme case study: Addis Ababa and surrounding catchment. M.Sc. thesis, Addis Ababa University, Ethiopia.

Abbaspour K.C, E.Rouholahnejad, R. Srinivasan, V. Bacu and A. Lehmann. (2014). Water resource of the Black Sea Basin at high spatial and temporal resolution. Water Resource. Res, 50(7), 5866-5885.

Abbaspour K.C, E.Rouholahnejad, S. Vaghefi, R. Srinivasan, H.Yang, B.Klove (2015). A continental-scale hydrology and water quality model for Europe: Calibration and uncertainity of a high-resolution large-scale SWAT model. Journal of Hydrology, 524, 733-752.

Abbaspour K. C. (2015). SWAT Calibration and Uncertainty Programs-A user manual. Eawag: Swiss Federal Institute of Aquatic Science and Technology.

Abraham M, Thomas W and S.Birk. (2015). Recharge variability and sensitivity to climate: the example of Gidabo river basin, main Ethiopia rift. Journal of hydrology: regional studies, 4, 644-660.

Abdo KS, Fiseha BM, Rientjes THM, Gieske ASM, Haile AT (2009) Assessment of climate change impacts on the hydrology of Gilgel Abay catchment in Lake Tana basin, Ethiopia. Hydrol Process 23: 3661-3669.

Akinsanola, A.A., Ogunjobi, K.O., 2017. Evaluation of present-day rainfall simulations over West Africa in CORDEX evaluation of present-day rainfall simulations over West Africa in CORDEX regional climate models, Environ. Earth Sci. 76 (366), 1–20. https://doi.org/10.1007/s12665-017-6691-9 .

Alemseged Tamiru Haile and Tom Rientjes, 2015. Evaluation of regional climate model simulations of rainfall over the Upper Blue Nile basin, Elsevier B.V.http://dx.doi.org/10.1016/j.atmosres.2015.03.013.

Alemu, A. 2011, Evaluation of climate change impact on extreme hydrological event, case study of Addis Ababa and surrounding. . Msc thesis, Addis Ababa University, Addis Ababa, Ethiopia.

Amba Shalishe, 2017. Evaluation of Climate Change Impacts on Run-Off in the Gidabo River Basin: Southern Ethiopia (https://www.researchgate.net

Arnold, J., Srinivasan, R., Muttiah, R., and Williams, J.: Large area hydrologic modeling and assessment – Part 1: Model development, J. Am. Water Resour. Assoc., 34, 73–89, 1998.

Asmamaw A. (2013). Assessing the impacts of land use and land cover change on hydrology of watershed: A case study on GILGEL-ABAY watershed, Lake Tana basin Ethiopia. MSC thesis, Consortium Universities, Washington.

Asselman N.E, H. Middelkoop and P.M. van Dijk. (2003). The impact of changes in climate and land use on soil erosion, transport and deposition of suspended sediment in the River Rhine. Hydrological Processes, 7, 3225-3244.

Bekele, 2009.Evaluation of climate change impact on upper Blue Nile basin reservoir. M.Sc. thesis, Arba Minch University, Arba Minch, Ethiopia. /publication/318980162

Bergstrom S. (1992). The HBV model-its structure and application. SMHI.

Bhuvandas, N., Timbadiya, P.V., Patel, P.L. and Porey, P.D., 2014. Review of Downscaling Methods in Climate Change and Their Role in Hydrological Studies.

Christensen, J. H. et al. in Climate Change 2007: The Physical Science Basis (eds Solomon, S., Qin, D. & Manning, M.) 847–940 (Cambridge Univ. Press, 2007).

Chong-yu Xu. (2002). Textbook of hydrologic models. Sweden: Uppsala university Department of Earth Sciences.

Choudhari K, B.Panigrahi, J.Chandra. (2014). Simulation of rainfall-runoff process using HEC-HMS model for Balijore Nala watershed, Odisha, India. International Journal of Geomatics and Geosciences.

Dibike, Y.B. and Coulibaly, P., 2005. Hydrologic impact of climate change in the Saguenay watershed: comparison of downscaling methods and hydrologic models. Journal of ydrology, 307(1), pp.145-163.

Diro, G.T., Toniazzo, T., Shaffrey, L., 2011. Ethiopian rainfall in climate models. Adv. Global Change Res. 43, 51 –69. https://doi.org/10.1007/978-90-481-3842-5_3

Elshamy, E., Seierstad, I. A., Sorteberg, A., (2009). Impacts of climate change on Blue Nile flows using bias-corrected GCM scenarios, Hydrol. Earth Syst. Sci., 13, 551–565.

Endris, H.S., et al., 2013. Assessment of the performance of CORDEX regional climate models in simulating east African rainfall. J. Clim. 26, 8453–8475. https://doi.org/10.1175/JCLI-D-12-00708.1.

Fasil G/M. (2012). Prediction of sediment inflow to Gefersa reservoir (using SWAT model) and assessing sediment reduction methods. Msc thesis, Addis Ababa University, Ethiopia.

Feser F, Rockel B, von Storch H, Winterfeldt J, Zahn M. 2011. Regional climate models add value to global model data: a review and selected examples. Bulletin of the American Meteorological Society 92 (9): 1181–1192

Gbobaniyi, E., et al., 2014. Climatology, annual cycle and interannual variability of precipitation and temperature in CORDEX simulations over West Africa.

Giorgi, F., Jones, C., Asrar, G.R., 2009. Addressing climate information needs at the regional level: the CORDEX framework. WMO Bulletin 58 (3), 175 –183.

Haile, A.T., Rientjes, T., 2015. Evaluation of regional climate model simulations of rainfall over the Upper Blue Nile basin. Atmos. Res. 161 –162, 57 – 64.https://doi.org/10.1016/j.atmosres.2015.03.013. Elsevier B.V.

IPCC, 2013 Summary for Policymakers In: Climate Change 2013: The Physical Science Basis. Contribution of Working Group I to the Fifth Assessment Report Intergovernmental Panel on Climate Change [Stocker, T.F., D. Qin, G.-K. Plattner, M. Tignor, S. K. Allen, J. Boschung, A. Nauels, Y. Xia, V. Bex and P.M. Midgley (eds.)]. Cambridge University Press,

IPCC, 2014: Climate Change 2014: Synthesis Report. Contribution of Working Groups I, II and III to the Fifth Assessment Report of the Intergovernmental Panel on Climate Change [Core Writing Team, R.K. Pachauri and L.A. Meyer (eds.)]. IPCC, Geneva, Switzerland, 151 pp.

Jajarmizadeh M, Sobri Harun and Mohsen Salarpour. (2012). A review on theoretical considerastion and types of models in hydrology. Journal of environmental science and technology, 5(5) 249-261.

Khalid K, M.F.Ali, N.F.Abd Rahman, and M.R. Mispan. (2016). Application on one-at-a-time sensitivity analysis of semi-distributed hydrological model in tropical watershed. IACSIT international journal of engineering.

Kim Jung-woo and pachepsky Yakov A. (2010). Reconstructing missing daily precipitation data using regression trees and ANN for SWAT streamflow simulation. Journal of hydrology, 305-314

Kassa, T (2009). Watershed Hydrological Responses to Changes in Land Use and Land Cover, and Management Practices at Hare Watershed, Ethiopia.

Keller, M. (2009): Climate Risks and Development Projects: Assessment Report for a Community-Level Project in Guduru, Oromiya, Ethiopia.

Li L, Li W, Ballard T, Sun G, Jeuland M. 2015. CMIP5 model simulations of Ethiopian Kiremt-season precipitation: current climate and future changes. Climate Dynamics 46 (9–10): 2883–2895 DOI: 10.1007/s00382-015-2737-4

Marvel, K. and Bonfils, C., 2013. Identifying external influences on global precipitation.Proceedings of the National Academy of Sciences, 110(48), pp.19301-19306.

Mearns, L. O. et al. in Climate Change 2001: The Physical Science Basis (Eds Houghton, J. T., Ding, Y. & Griggs, D. J.) 739–768 (Cambridge Univ. Press, 2001).

Meehl, G. A. et al. Decadal prediction: can it be skillful? Bull. Am. Meteorol. Soc. 90, 1467–1485 (2009).)

Taylor KE, Stouffer RJ, Meehl GA (2011). An overview of CMIP5 and the experiment design. Bull Am Meteorol Soc 93: 485-498.].

McSweeney, C.; New, M.; Lizcano, G. (2008): UNDP Climate Change Country Profiles: Ethiopia. http://ncsp.undp.org/sites/default/files/Ethiopia.oxford.report.pdf

Ministry of Water, Irrigation and Electricity (MoWIE) Environmental Impact Assessment Report for Gidabo Irrigation Project Reviewed and updated. Addis Ababa, Ethiopia, 2019

Moriasi DN, Arnold JG, Van Liew MW, Bingner RL, Harmel RD, VeithTL. 2007. Model Evaluation Guidelines for Systematic Quantification of Accuracy in Watershed Simulations. American Society of Agricultural and Biological Engineers 50(3): 885–900.

Nemec J. (1993). Comparison and selection of existing hydrological models for the simulation of the dynamic water balance processes in basins of different sizes and on different scales. CHR.

Neitsch S.L, Arnols J.G, Kiniry J.R, Williams J.R. (2011). Soil and water assessment tool theoretical documentation. Texas A&M University.

Nigatu, Z.M. 2013. Hydrological impact of climate change on Lake Tana water balance M.Sc. thesis, International Institute for Geo-information science and Earth observation, Netherlands

Pechlivanidis Jackson, Mcintyre, Wheater. (2011). Cathment scale hydrological modelling: a review of model types, calibration approaches and uncertainity analysis methods in the context of recent development in technology and application. Global NEST journal, 193-214.

Perry, K. (2015). Application of the SWAT hydrological model in a small, mountainous catchment in South Africa. MSC thesis, University of Pretoria, South Africa

Pielke R. 2002. Mesoscale meteorological modeling. Elsevier, Amsterdam.

Reda, D.T., et al., 2015. Analysis of precipitation based on ensembles of regional climate model simulations and observational databases over Ethiopia for the period1989 – 2008. Int. J. Climatol. 35, 948 –971. https://doi.org/10.1002/joc.4029.

Moss, R., Edmonds, J., Hibbard, K. *et al.* The next generation of scenarios for climate change research and assessment. *Nature* **463,** 747–756 (2010). https://doi.org/10.1038/nature08823

Rientjes, Steenhuis et al. (2011). Changes in land cover, rainfall and streamflow in Upper Gilgel Abbay catchment, Blue Nile basinEthiopia. Hydrol Earth Syst Sci. , 15: 1979-1989. https://doi.org/10.5194/hess-15-1979-2011

Seibert, J. (2002) HBV light: version 2 user's manual. Department of Earth Sciences, Hydrology, Uppsala University, Sweden.

Sen, P. K. (1980). Estimates of the regression coefficient based on Kendall‘s tau. Journal of the American Statistical Association. 63(324), 1379–1389. http://dx.doi.org/10.1080/01621459.1968.10480934

Singh V, N. Bankar, S. S.Salunkhe, A.K. Bera and J.R.Sharma. (2013). Hydrological stream flow modelling on Tungabhadra catchment: parameterization and uncertainty analysis using SWAT CUP. Current science, 104(9), 1187-1199.

Teutschbein, C. and Seibert, J.: Bias correction of regional climate model simulations for hydrological climate-change impact studies: Review and evaluation of different methods, J. Hydrol., 456, 12–29, doi:10.1016/j.jhydrol.2012.05.052, 2012.

Van Vuuren, D. (2011). RCP2.6: Exploring the possibility to keep global mean temperature change below 20C. . Climatic Change, 109: 95–116. doi:10.1007/s10584-011-0152-3

Winchell M, R. Srinivasan, M. Di Luzio, J. Arnold. (2013). ARCSWAT INTERFACE FOR SWAT2012. Texas: USAD Agricultural research service.

Xu, C. Y. (1999). From GCMs to river flow: a review of downscaling methods and hydrologic modelling approaches. *Progress in Physical Geography, 23(2)*, 229-249.

Zelalem C, 2013. Downscaling and modeling the effects of climate change on hydrology and water resources in the upper Blue Nile river basin, Ethiopia. PhD dissertation, university of Kassel, Germany.

Zheng J, Ge Sun, Wenhong Li, Xinxiao Yu, Chi Zhang, Yuanbo Gong and Lihua Tu. (2016). Impacts of Land use change and climate variations on annual inflow into Miyun Reservoir, Beijing, China. Hydrology and Earth System Sciences, 20(4), 1561-1572.

APPENDIX

Appendix I: Homogenization result using *Rclimatol* package for maximum temperature

Appendix Figure 1: Box-plots of the data at every station (left) and histogram of all data (right)

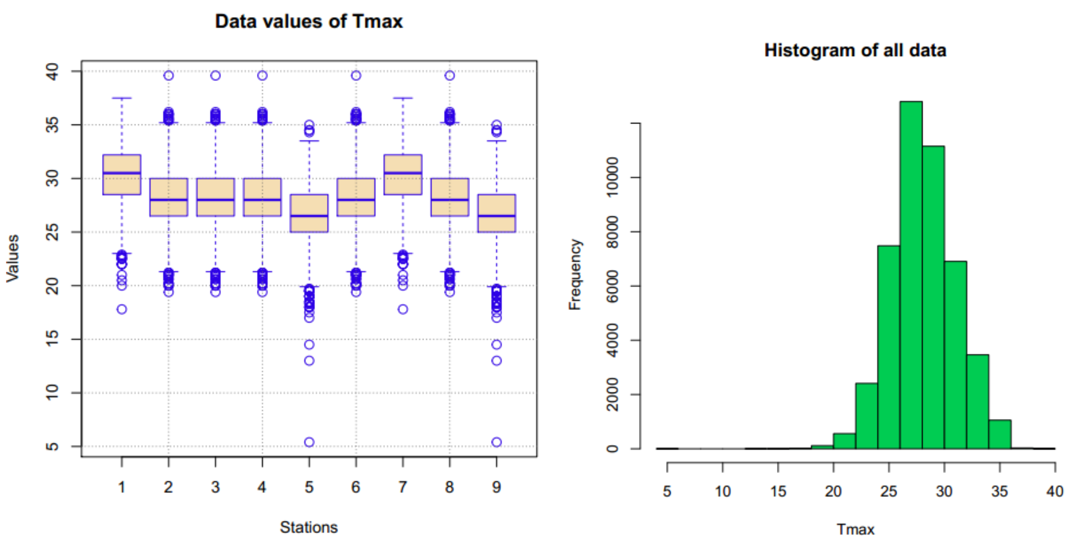

Appendix Figure 2: Correlogram of the series (left) and map of the stations (right; colors identify groups of stations with similar variability)

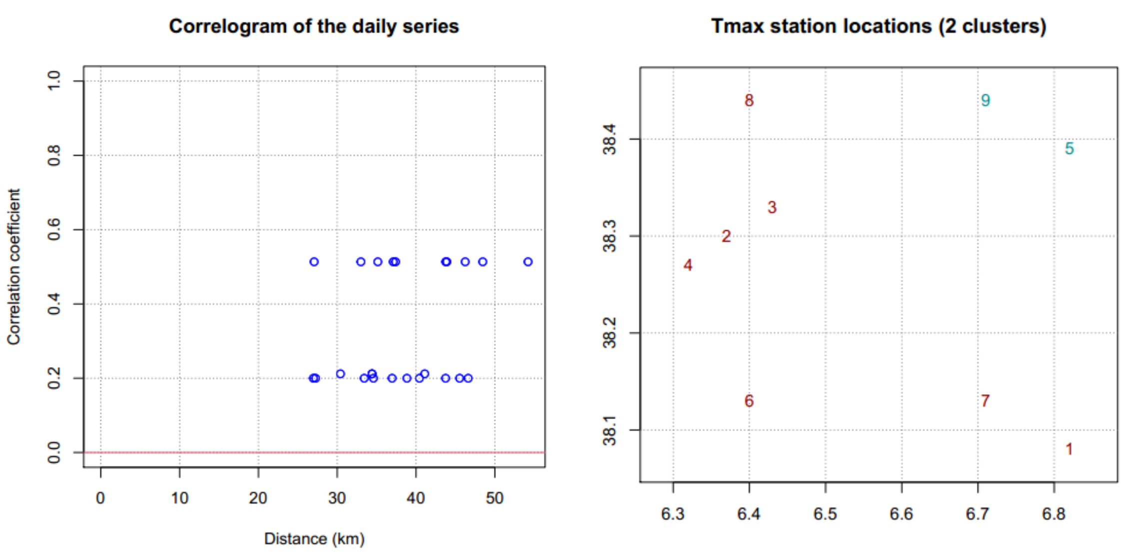

Appendix Figure 3: Anomalies of a homogeneous series (left) and a very inhomogeneous one (right)

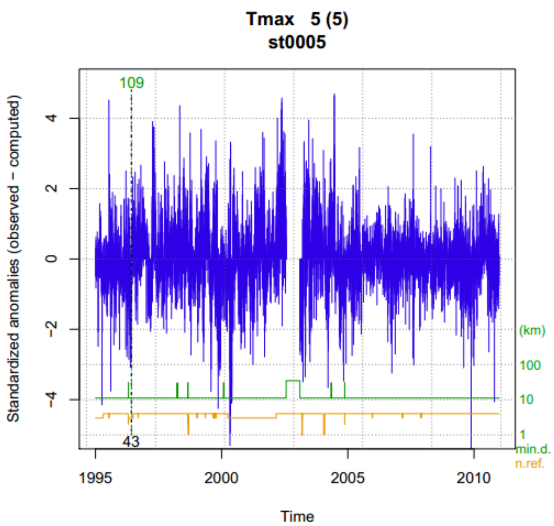

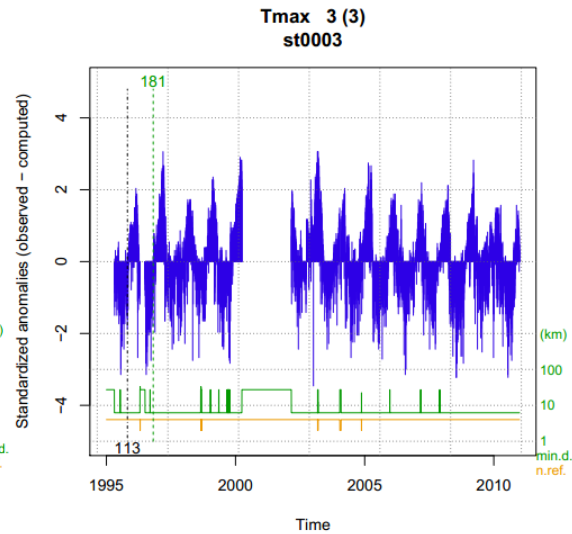

Appendix Figure 4: Histogram of anomalies (all data together)

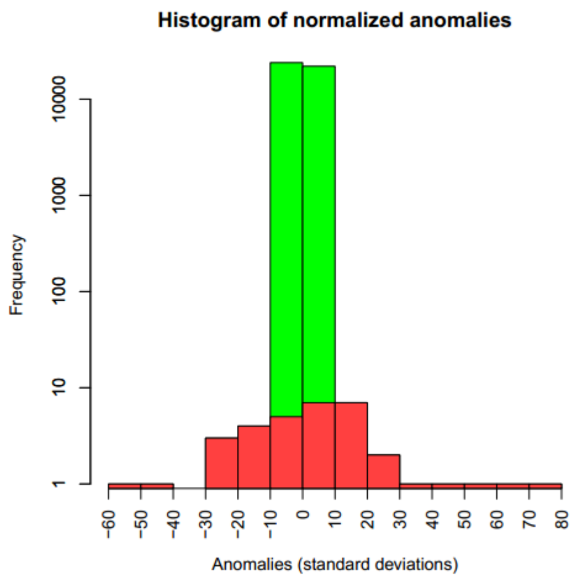

Appendix Figure 5: Histograms of the maximum SNHT values found on overlapping stepped windows (left) and on the whole series (right)

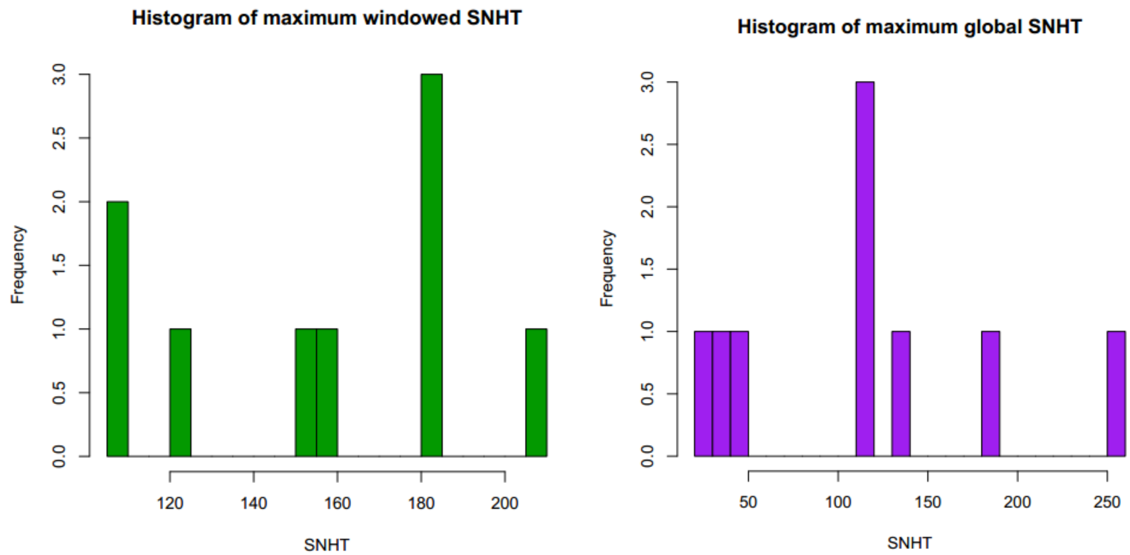

Appendix Figure 6: Quality/singularity plot of the final series

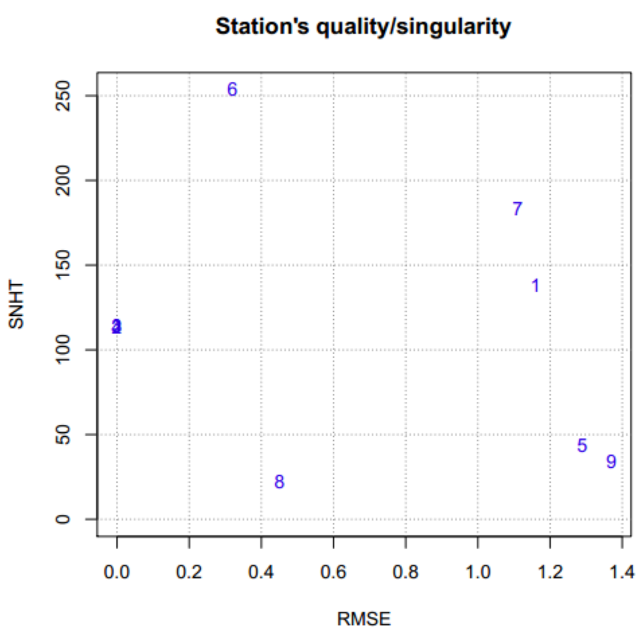

Appendix II: Homogenization result using *Rclimatol* package for precipitation

Appendix Figure 7: Box-plots of the data at every station (left) and histogram of all data (right)

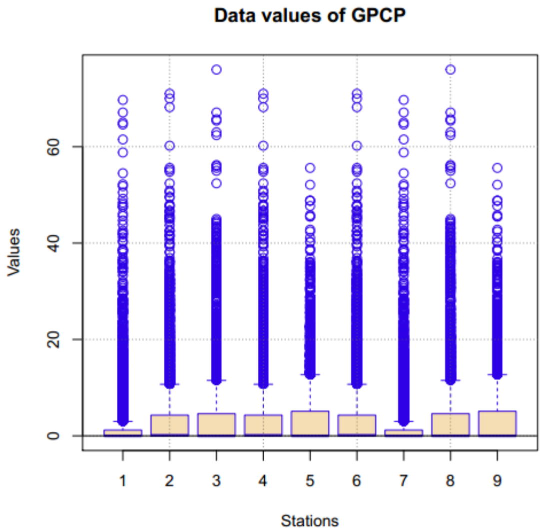

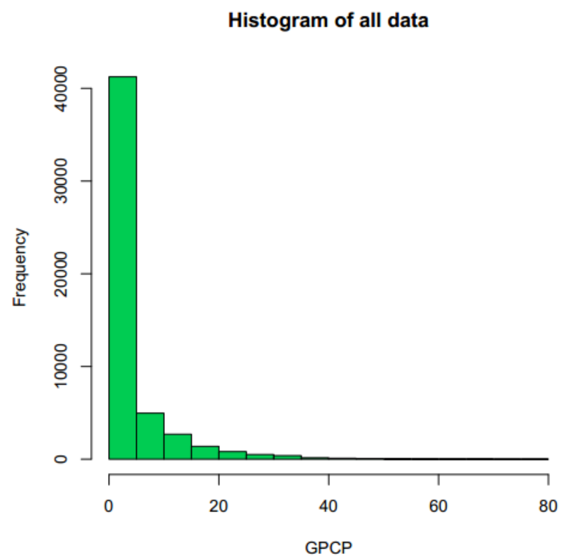

Appendix Figure 8: Correlogram of the series (left) and map of the stations (right; colors identify groups of stations with similar variability)

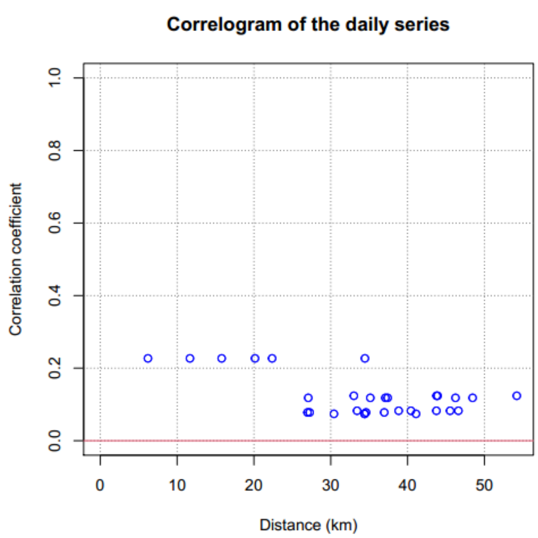

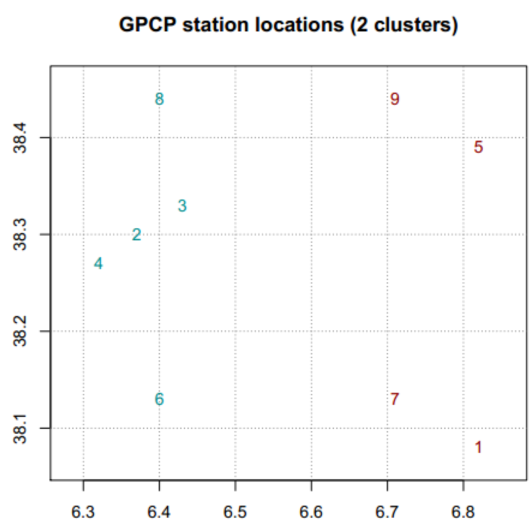

Appendix Figure 9: Histogram of anomalies (all data together)

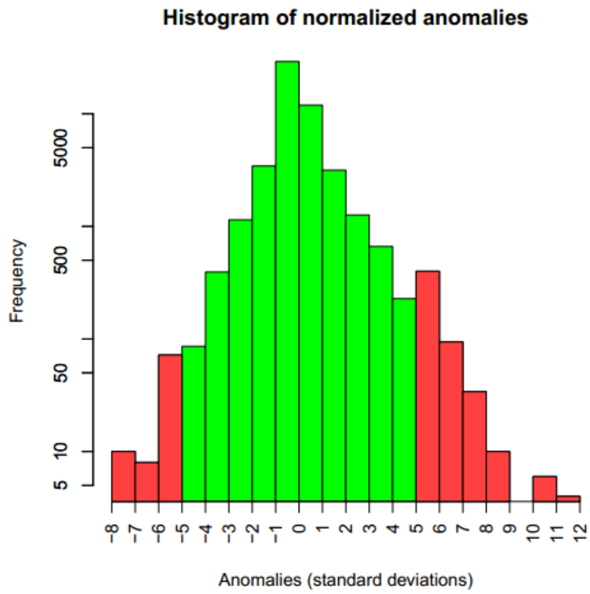

Appendix Figure 10: Histograms of the maximum SNHT values found on overlapping stepped windows (left) and on the whole series (right)

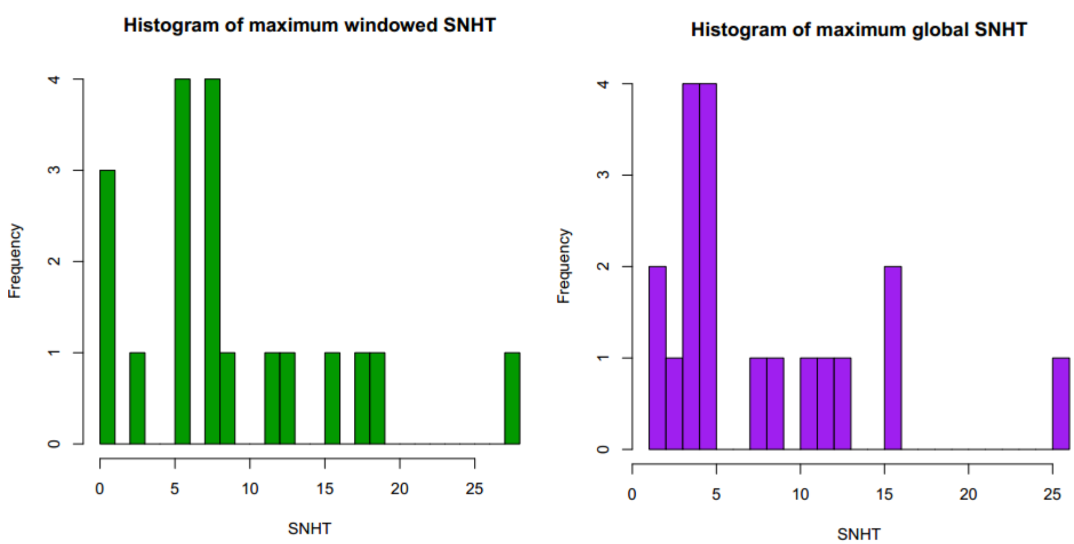

Appendix Figure 11: Quality/singularity plot of the final series

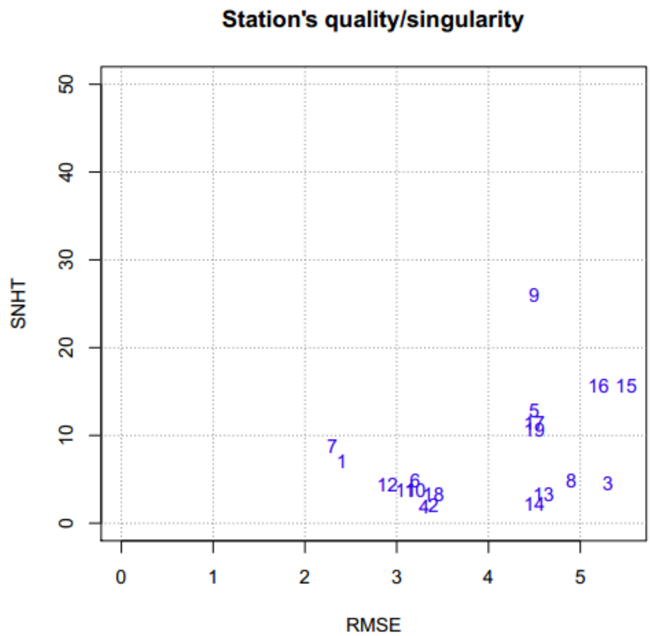

Appendix III: Homogenization result using *Rclimatol* package for minimum temperature

Appendix Figure 12: Box-plots of the data at every station (left) and histogram of all data (right)

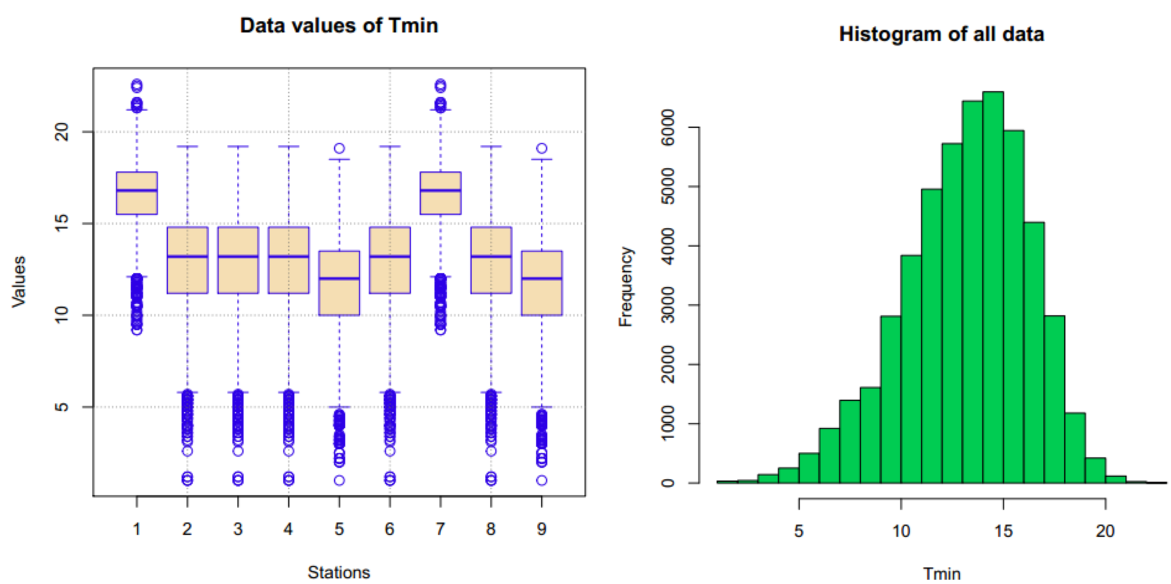

Appendix Figure 13: Correlogram of the series (left) and map of the stations (right; colors identify groups of stations with similar variability).

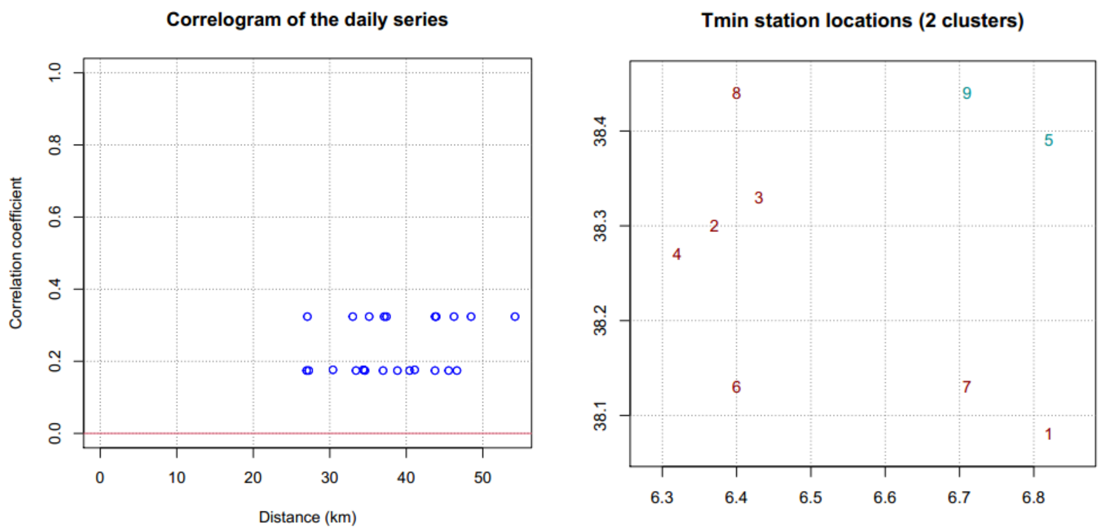

Appendix Figure 14: Anomalies of a homogeneous series (left) and a very inhomogeneous one (right)

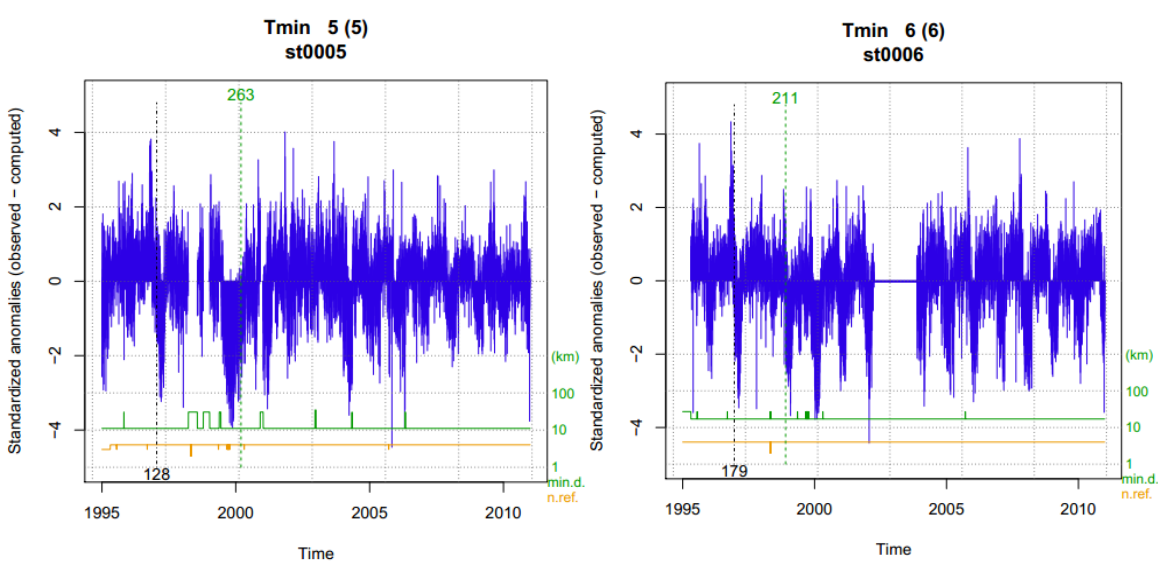

Appendix Figure 15: Histogram of anomalies (all data together)

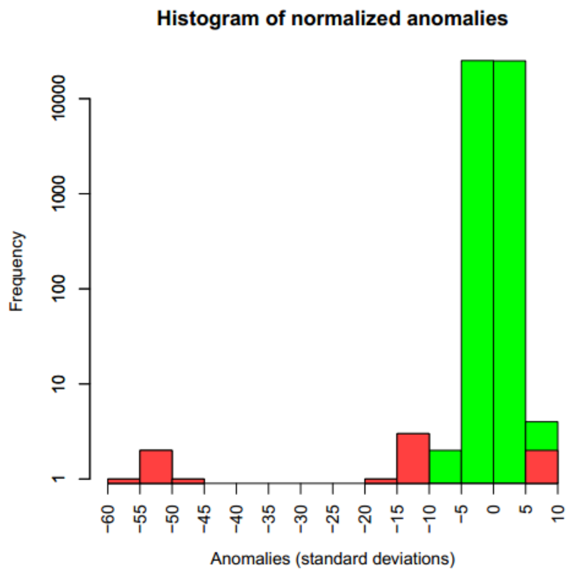

Appendix Figure 16: Histograms of the maximum SNHT values found on overlapping stepped windows (left) and on the whole series (right).

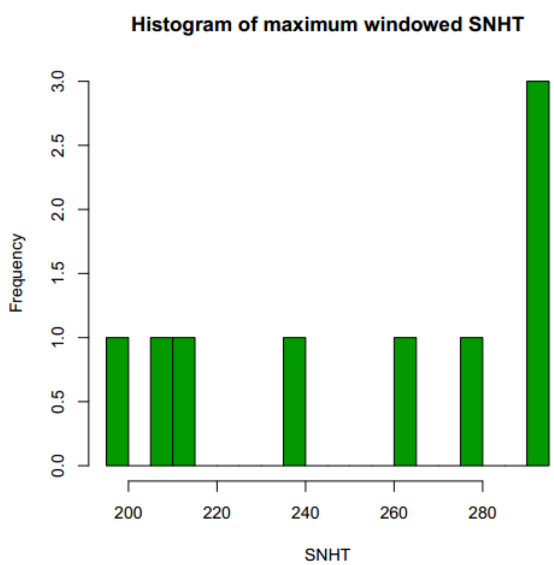

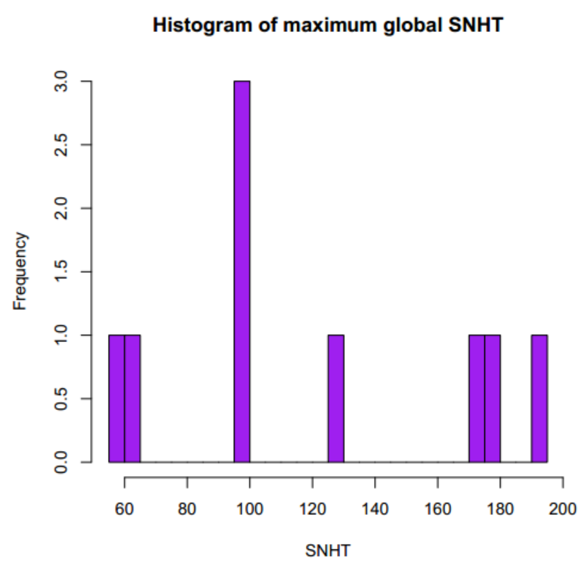

Appendix Figure 17: Quality/singularity plot of the final series

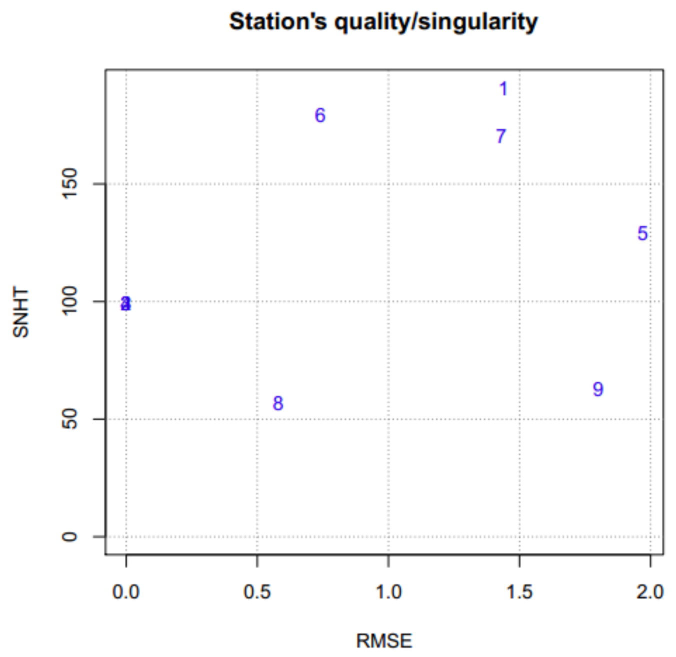

Appendix IV: Definition of weather generator statics and probability value symbol

TMPMX: Average or mean daily maximum air temperature for month (°C)

TMPMN: Average or mean daily minimum air temperature for month (°C)

TMPSTDMX: Standard deviation for daily maximum air temperature for month (°C)

TMPSTDMN: Standard deviation for daily minimum air temperature for month (°C)

PCPMM: Average or mean total monthly precipitation (mm H2O)

PCPSTD: Standard deviation for daily precipitation for month (mm H2O/day)

PCPSKW: Skew coefficient for daily precipitation in month

PR_W1: Probability of a wet day following a dry day in the month

PR_W2: Probability of a wet day following a wet day in the month

PCPD: Average number of days of precipitation in month

SOLARAV: Average daily solar radiation for month (MJ/m2/day)

DEWPT: Average daily dew point temperature in month (^oC)

WNDAV: Average daily wind speed in month (m/s)

Appendix V: Weather generator statistic and probability values

Appendix Table1: Dilla station

	Jan	Feb	Mar	Apr	May	Jun	Jul	Aug	Sep	Oct	Nov	Dec
TMPMX	30.15	31.46	30.98	28.63	27.34	26.56	25.72	26.19	26.47	27.06	28.37	29.21
TMPMN	10.59	10.72	12.57	13.91	13.76	13.66	14.22	14.17	13.67	13.50	11.61	10.18
TMPSTMX	1.54	1.84	2.47	2.11	1.87	1.56	1.81	1.54	1.43	1.76	1.40	1.26
TMPSTDMN	3.02	3.16	2.43	1.68	1.78	1.77	1.76	1.81	1.72	1.95	2.35	2.97
PCPMM	39.19	28.81	91.06	193.06	194.31	94.19	78.75	109.38	142.69	147.00	55.50	32.19
PCPSTD	3.81	3.60	6.00	8.65	8.33	6.22	6.30	6.35	6.50	6.82	4.40	3.31
PCPSKW	4.12	5.27	2.66	1.76	1.91	2.72	4.23	2.36	1.85	2.03	3.20	4.94
PR_W(1)	0.12	0.14	0.27	0.55	0.59	0.36	0.30	0.45	0.52	0.40	0.19	0.13
PR_W(2)	0.51	0.39	0.51	0.67	0.71	0.47	0.44	0.47	0.70	0.74	0.52	0.43
PCPD	5.94	5.19	11.13	18.69	20.69	12.06	10.75	14.25	19.00	18.75	8.63	5.56
RAINHHMX	4.42	3.94	6.73	10.29	10.21	7.94	8.54	7.35	8.13	8.48	5.75	3.48
SOLARAV	21.17	23.51	22.24	21.03	18.54	16.87	14.73	16.24	18.17	18.97	22.70	22.00
DEWPT	0.50	0.43	0.56	0.76	0.85	0.86	0.86	0.84	0.83	0.83	0.68	0.55
WINDAV	2.03	2.18	2.27	2.12	2.00	1.99	1.98	1.98	2.03	1.97	2.01	2.04

Appendix Table2: Yirgalem station

	Jan	Feb	Mar	Apr	May	Jun	Jul	Aug	Sep	Oct	Nov	Dec
TMPMX	28.27	29.19	28.93	27.52	26.13	25.35	23.85	24.54	24.92	25.73	26.74	27.28
TMPMN	10.26	10.62	11.33	12.37	12.74	12.58	13.08	12.81	12.16	11.74	9.93	9.34
TMPSTMX	1.56	1.58	1.85	2.05	2.59	1.98	1.87	1.66	1.51	1.87	1.70	1.48
TMPSTDMN	2.75	2.54	2.49	2.49	1.92	1.74	1.65	2.13	2.31	2.42	2.75	2.71
PCPMM	36.25	21.38	85.50	151.69	138.50	89.19	89.25	103.56	112.00	127.88	38.50	30.50
PCPSTD	3.38	2.85	4.91	6.86	6.37	5.37	5.98	5.32	5.50	6.78	3.98	3.22
PCPSKW	3.87	5.45	2.35	1.86	2.09	2.71	3.17	1.99	1.98	2.27	3.81	4.55
PR_W(1)	0.12	0.07	0.26	0.38	0.39	0.35	0.28	0.33	0.38	0.19	0.09	0.08
PR_W(2)	0.43	0.45	0.60	0.67	0.63	0.44	0.49	0.55	0.56	0.73	0.43	0.46
PCPD	5.44	3.31	12.31	16.00	15.81	11.44	11.00	13.06	13.88	12.94	4.25	4.19
RAINHHMX	3.71	3.10	5.23	7.73	8.00	6.00	7.58	6.10	6.17	7.38	4.56	3.15
SOLARAV	21.93	23.83	23.00	22.77	22.56	20.18	18.09	19.31	21.17	22.09	23.16	22.34
DEWPT	0.45	0.39	0.50	0.67	0.76	0.79	0.80	0.78	0.77	0.74	0.60	0.49
WINDAV	1.93	2.04	2.00	1.82	1.84	1.96	1.97	1.92	1.81	1.71	1.79	1.86

Appendix VI: Soil parameters of the study area used in the SWAT model

OBJECTID	MU_SOURCE1	TEXTURE	Value	%	Shape_Area	HYDGRP
1	ET1013	Loam	1	3.22	84.88	A
2	ET1064	Clay Loam	3	26.36	694.82	A
3	ET1103	Clay Loam	4	7.30	192.31	A
4	ET1128	Sandy Caly Loam	5	13.47	355.11	B
5	ET1138	Sandy Caly Loam	7	21.30	561.48	B
6	ET1154	Sandy Caly Loam	8	6.52	171.83	B
7	ET1183	Clay	9	0.45	11.77	B
8	ET1187	Clay	10	0.27	7.24	B
9	ET1204	Clay	12	0.05	1.33	B
10	ET1214	Clay	13	0.39	10.34	B
11	ET1270	Clay	17	0.34	8.99	D
12	ET1276	Clay	18	10.54	277.79	D
13	ET1282	Clay	19	9.78	257.86	D

Appendix VII: Calibration outputs

AVE MONTHLY BASIN VALUES

MON	RAIN (MM)	SNOW FALL (MM)	SURF Q (MM)	LAT Q (MM)	WATER YIELD (MM)	ET (MM)	SED YIELD (T/HA)	PET (MM)
1	36.19	0.00	0.78	1.52	10.57	28.27	0.09	159.61
2	26.42	0.00	0.82	1.19	4.53	28.56	0.10	163.48
3	84.53	0.00	2.32	1.86	6.39	65.79	0.09	170.71
4	142.81	0.00	5.96	3.69	14.26	89.85	0.15	142.16
5	153.24	0.00	10.14	6.23	31.81	88.17	0.20	129.60
6	85.03	0.00	4.06	4.75	32.29	61.90	0.07	115.39
7	79.85	0.00	4.90	3.37	30.16	51.26	0.12	107.93
8	104.01	0.00	5.78	3.90	29.84	63.34	0.10	115.84
9	116.85	0.00	5.98	4.08	32.04	66.88	0.08	119.98
10	136.37	0.00	11.21	5.84	47.36	71.45	0.26	127.81
11	40.22	0.00	1.73	3.90	38.81	56.64	0.08	143.07
12	31.90	0.00	0.96	2.05	22.60	42.31	0.08	154.12

AVE ANNUAL BASIN STRESS DAYS

WATER STRESS DAYS = 11.15

TEMPERATURE STRESS DAYS = 9.91

NITROGEN STRESS DAYS = 132.61

PHOSPHORUS STRESS DAYS = 0.25

AERATION STRESS DAYS = 0.00

SWAT Sep 7 VER 2018/Rev 670

General Input/Output section (file.cio):
3/14/2021 12:00:00 AM ARCGIS-SWAT interface AV

```
     AVE ANNUAL BASIN VALUES

          PRECIP =   1037.6 MM
          SNOW FALL =    0.00 MM
          SNOW MELT =     0.00 MM
          SUBLIMATION =     0.00 MM
          SURFACE RUNOFF Q =    54.66 MM
          LATERAL SOIL Q =   42.38 MM
          TILE Q =     0.00 MM
          GROUNDWATER (SHAL AQ) Q =   191.94 MM
          GROUNDWATER (DEEP AQ) Q =    11.73 MM
          REVAP (SHAL AQ => SOIL/PLANTS) =   30.16 MM
          DEEP AQ RECHARGE =    11.57 MM
          TOTAL AQ RECHARGE =  231.49 MM
          TOTAL WATER YLD =   300.70 MM
          PERCOLATION OUT OF SOIL =  229.89 MM
          ET =    714.6 MM
          PET =   1651.1MM
          TRANSMISSION LOSSES =     0.00 MM
          SEPTIC INFLOW =       0.00 MM
          TOTAL SEDIMENT LOADING =      1.41 T/HA
          TILE FROM IMPOUNDED WATER =     0.000 (MM)
          EVAPORATION FROM IMPOUNDED WATER =     0.000 (MM)
          SEEPAGE INTO SOIL FROM IMPOUNDED WATER =    0.000 (MM)
          OVERFLOW FROM IMPOUNDED WATER =    0.000 (MM)

SWAT Sep 7    VER 2018/Rev 670

General Input/Output section (file.cio):
3/14/2021 12:00:00 AM ARCGIS-SWAT interface AV
```

Dotty plot

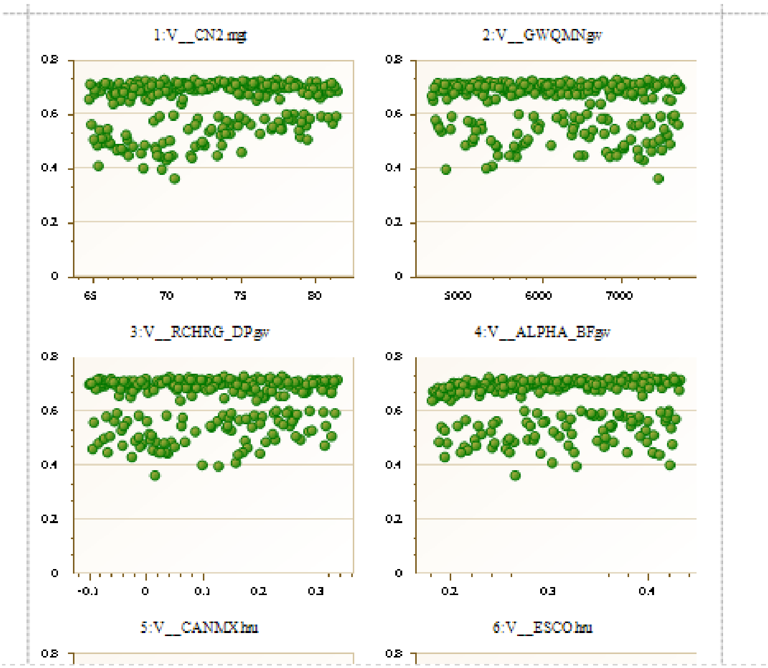

1:V__CN2.mgt
2:V__GWQMN.gw
3:V__RCHRG_DP.gw
4:V__ALPHA_BF.gw
5:V__CANMX.hru
6:V__ESCO.hru

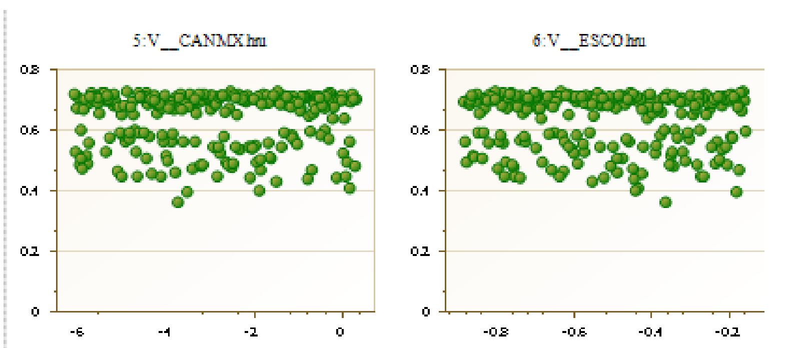

5:V__CANMX.hru
6:V__ESCO.hru

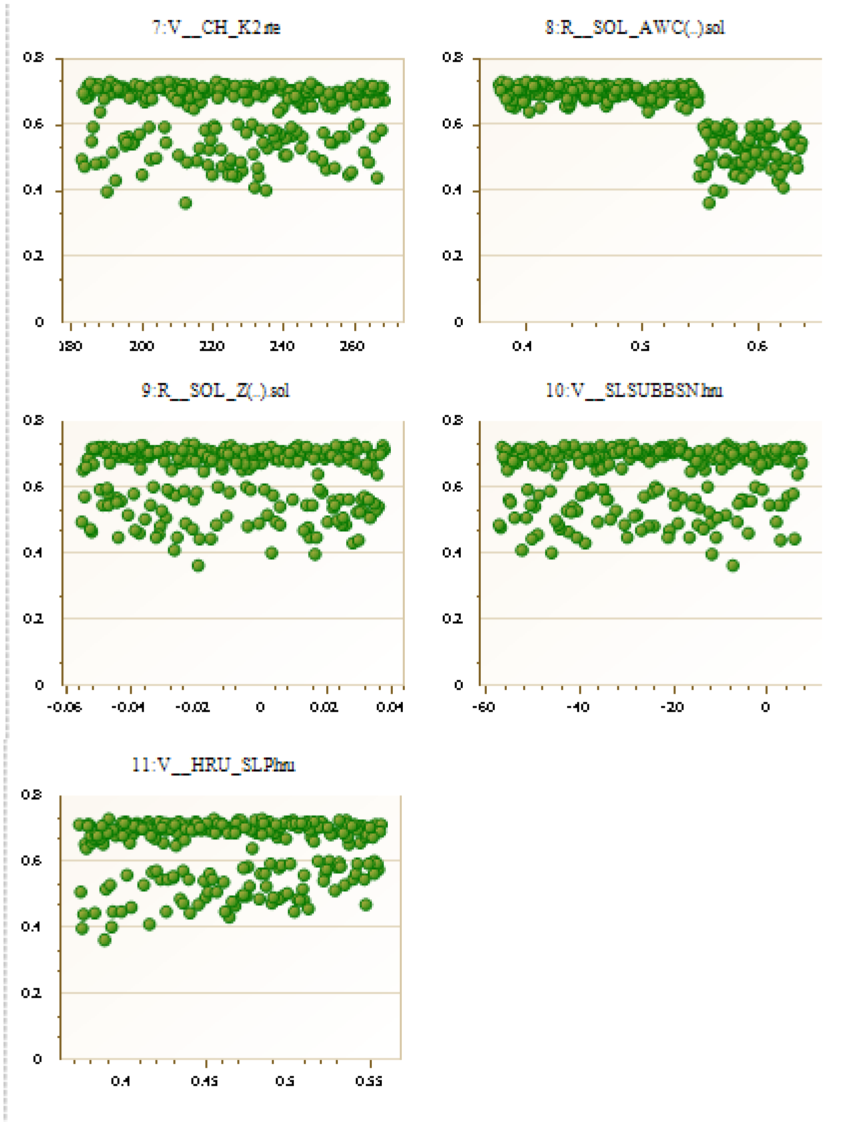
7:V__CH_K2.rte
8:R__SOL_AWC(..).sol
9:R__SOL_Z(..).sol
10:V__SLSUBBSN.hru
11:V__HRU_SLP.hru
0.8
0.6
0.4
0.2
0
180 200 220 240 260
0.4 0.5 0.6
-0.06 -0.04 -0.02 0 0.02 0.04
-60 -40 -20 0
0.4 0.45 0.5 0.55

Appendix VIII: Monthly mean stream flows of Gidabo River Catchment in period of 1998 - 2010

Appendix Table 3: Stream flow (m^3/s) in Aposto station

year	Jan	Feb	Mar	Apr	Mar	June	July	Aug	Sep	Oct	Nov	Dec
1998	2.06	1.05	1.19	3.34	10.10	4.48	7.58	8.14	10.93	25.75	6.11	2.73
1999	2.17	1.74	1.91	1.91	3.67	2.47	2.47	3.07	3.95	6.83	2.99	1.89
2000	1.41	1.30	1.27	1.96	4.91	3.02	2.51	7.83	7.20	6.48	3.27	2.45
2001	2.24	1.81	1.90	2.77	5.63	6.36	3.93	3.81	6.92	12.83	4.14	2.48
2002	2.01	1.56	2.04	2.93	3.94	5.29	2.71	3.66	4.89	3.53	2.19	2.24
2003	1.84	1.47	1.71	4.02	2.99	2.40	3.01	6.55	4.84	7.93		
2004					3.45	3.24	2.79	4.02	6.21	7.94	2.62	2.17
2005	1.77	1.37	1.72	2.84	10.53	6.76	5.56	6.01	8.78	6.27	3.67	2.02
2006	1.65	1.67	2.75	4.56	9.25	5.27	10.96	13.93	8.87	10.99	6.37	4.54
2007	3.04	2.53	2.29	4.96	9.96	10.62	7.16	16.72	11.62	10.91	4.08	2.51
2008	2.01	1.73	1.53	2.00	3.43	4.06	4.34	5.47	6.20	6.25	12.78	2.93
2009	2.36	2.22	1.74			3.46	2.71	3.60	5.03	8.23	2.99	3.51
2010	3.41	2.79	5.74	10.93	13.41	6.20	8.29	9.55	13.84	7.86	3.51	2.41

Appendix Table 4: Stream flow (m3/s) in Measso(Gidabo River Catchment outlet)

year	Jan	Feb	Mar	Apr	Mar	June	July	Aug	Sep	Oct	Nov	Dec
1998	19.53	16.81	14.44	20.52	58.05	26.50	33.64	35.31	30.70	65.25	40.69	12.10
1999	8.94	6.80	8.44	10.27	30.86	12.66	14.30	17.30	19.88	35.12	25.41	10.33
2000	6.80	5.51	4.08	6.23	32.66	26.91	13.51	20.51	30.74	32.14	32.48	15.31
2001	12.06	8.63	8.24	18.82	29.66	41.26	19.47	20.99	30.73	57.03	47.08	15.70
2002	9.11	6.28	8.67	30.36	29.54	32.24	13.43	17.45	24.48	29.20	13.44	11.48
2003	18.28	6.48	6.94	17.24	16.67	19.46	25.34	25.32	17.27			
2004					15.31	18.91	12.76	20.54	25.73	20.93	16.91	10.57
2005	7.78	5.65	6.89	17.30	52.18	32.02	24.40	26.59	48.43	44.95	32.75	9.05
2006	6.78	6.73	10.70	25.37	43.86	24.21	45.88	62.11	37.59	54.13	31.39	20.57
2007	13.68	10.63	9.11	19.53	48.59	64.02	36.60	73.13	68.88	61.25	22.75	12.30
2008	8.97	7.18	6.40	8.71	15.87	23.15	22.49	31.21	34.37	32.89	64.58	12.97
2009	9.68	8.83				11.23	11.16	19.03	25.30	38.25	12.43	13.51
2010	12.90	10.97	25.69	50.59	90.52	32.50	39.67	49.44	99.87	45.28	15.57	9.03

Appendix Table 5: Stream flow (m3/s) in Bedessa station

year	Jan	Feb	Mar	Apr	Mar	June	July	Aug	Sep	Oct	Nov	Dec
1998	3.41	1.98	0.89	2.41	4.47	2.94	1.84	2.98	1.87	3.60	1.64	0.65
1999	0.33	0.16	0.45	0.97	1.89	1.08	1.54	1.78	1.62	3.80	3.28	1.00
2000	0.50	0.24	0.15	0.34	5.28	1.16	1.27	2.67	2.80	4.32	2.82	1.83
2001	1.14	0.60	0.40	0.82	2.68	3.20	1.52	2.35	4.17	3.14	3.88	0.80
2002	0.54	0.20	0.39	0.53	3.33	2.74	1.05	1.23	1.96	1.65	1.58	0.97
2003	0.76	0.35	0.23	0.81	1.68	3.04	1.29	1.85				
2004				1.24	4.06	2.05	0.79	1.73	3.51	2.68	2.12	0.79
2005	0.40	0.21	0.21	0.32	4.09	2.21	1.27	1.43	2.78	4.32	2.70	0.51
2006	0.25	0.22	0.25	2.54	3.13	3.49	1.88	3.46	1.66	4.17	2.42	1.22
2007	0.79	0.44	0.27	0.51	3.64	7.31	3.09	3.76	5.67	6.24	2.29	0.93
2008	0.51	0.28	0.26	0.43	1.02	2.43	1.96	3.26	3.42	2.96	3.73	0.70
2009	0.35	0.26	0.14			0.64	0.41	1.73	2.05	2.48	0.49	0.27
2010	0.20	0.28	1.45	3.23	5.94	2.90	2.82	4.29	3.13	4.82	0.85	0.12